UCGE Reports
Number 20160

Department of Geomatics Engineering

Acceleration Estimation from GPS Carrier Phases for Airborne Gravimetry

(URL: http://www.geomatics.ucalgary.ca/links/GradTheses.html)

by

Sandra L. Kennedy

May 2002

UNIVERSITY OF CALGARY

Acceleration Estimation from GPS Carrier Phases for Airborne Gravimetry

by

Sandra L. Kennedy

A THESIS

SUBMITTED TO THE FACULTY OF GRADUATE STUDIES

IN PARTIAL FULFILLMENT OF THE REQUIREMENTS FOR THE

DEGREE OF MASTER OF SCIENCE IN GEOMATICS ENGINEERING

DEPARTMENT OF GEOMATICS ENGINEERING

CALGARY, ALBERTA

MAY, 2002

© Sandra L. Kennedy

Abstract

Accelerations derived from GPS are usually derived by twice time differentiating positions. In airborne gravimetry, the accuracy of accelerations obtained this way is limiting the achievable accuracy and resolution of the measured gravity field. Therefore, alternative methods of acceleration estimation need to be investigated. The current process, referred as the position method herein, has operation constraints, in addition to being unable to supply the desired accuracy.

An alternative method, referred to as the carrier method, is developed, implemented and evaluated. The carrier method estimates acceleration directly from the carrier phase measurements. A covariance model is developed and applied in the carrier method estimation process.

Testing is conducted using data from an airborne gravimetry campaign flown near Ottawa, Canada in the spring of 2000. An independent reference gravity field is available for the test area. Both methods of acceleration determination are used to estimate scalar gravity disturbances for approximately 720 km of flight lines.

Based on the analysis of the results, the carrier method offers a slight improvement (approximately 15% at 1.4 km resolution) in overall accuracy, as compared to the position method. In terms of robustness under operational conditions, the carrier method is shown to be better than the position method. Namely, positioning accuracies can be relaxed to the order of meters and changes in the visible GPS constellation do not adversely affect the estimated accelerations.

Acknowledgements

I thank Dr. K.P. Schwarz for supervising my graduate studies, and for providing a wonderful example of how to work and live.

I am very grateful for the financial support provided by the Natural Sciences and Engineering Research Council, iCORE, the GEOIDE Network of Excellence, the Department of Geomatics Engineering Graduate Research Scholarships and the Alberta Heritage Scholarship. This funding made my graduate studies possible.

Sander Geophysics is acknowledged for providing the NovAtel GPS data and reference gravity field used in my testing. Dr. El-Sheimy is also thanked for loaning me the GrafNav™ key.

I'm happy to have shared my time in graduate studies with my officemates and colleagues. Thanks to Michael Kern, Rob Radovanovic, Cameron Ellum, Sameh Nassar, Eun Hwan Shin, Bruce Wright, Alex Bruton, Kyle O'Keefe, and many others, for the many discussions, debates, and coffee breaks.

On a more personal note, I am more grateful than I can express for my dedicated and loving parents, Dulcie and Alan. They built the foundation of work ethic and self-reliance that has brought me this far.

Lastly, but most dearly, I thank my husband Arlin for his unwavering support and encouragement.

Table of Contents

List of Tables

List of Figures

Notation, Symbols and Acronyms

Notation

Vectors and matrices are bold typeface, while scalars are normal typeface. Dots above a variable indication time differentiation. The remote (roving) receiver is referred to as receiver 'm', and the base (static) receiver is receiver 'k'.

Symbols

Symbols are defined as they are used within the text. Commonly used symbols are given below for quick reference.

δg gravity disturbance

δg_u gravity disturbance in the upward direction

ϕ_m^p carrier phase measurement from satellite 'p' to receiver 'm'

ρ_m^p geometric range from satellite 'p' to receiver 'm'

$\mathbf{e}_m^p$ unit direction vector from receiver 'm' to satellite 'p'

$\mathbf{x}_m^p$ relative position vector from receiver 'm' to satellite 'p'

$\dot{\mathbf{x}}_m^p$ relative velocity vector from receiver 'm' to satellite 'p'

$\ddot{\mathbf{x}}_m$ receiver antenna acceleration

Acronyms

The following acronyms are used frequently. Their corresponding meanings are given below.

C/No	Carrier to noise ratio, measured by the receiver for GPS carrier phase measurements
DGPS	Differential Global Positioning System, referring the technique of differencing GPS measurements to reduce correlated errors
FIR	Finite Impulse Response
IF	Ionospheric Free

GNSS	Global Navigation Satellite System
GPS	Global Positioning System
GREATGUN	Gravity Estimates from Airborne Techniques for Geoidal Undulations, a software package developed at the University of Calgary
INS	Inertial Navigation System
L1, L2	GPS carrier signals
LCR	LaCoste Romberg
PRN	Pseudo Random Number, used to identify GPS satellites
SP3	file format of precise ephemeris for GPS satellites

Chapter 1

Introduction

Knowledge of the gravity field is valuable in many scientific areas. Geodesy, geophysics, and oceanography use the gravity field to measure heights, to reflect the Earth's interior, and to study the movement of water in the oceans. Gravity measurement techniques have progressed from terrestrial point measurements, to shipborne measurements, to deriving gravity from the perturbations of satellite orbits, and most recently to airborne gravity measurements. As the capabilities of the measurement techniques increase, the demand for higher accuracy and resolution also increases, although it is tempered by operational constraints such as the cost and time required to obtain gravity information. Airborne gravimetry is a comparatively economical and efficient measurement technique, which can be employed anywhere aircraft can fly. It is well suited to large, inaccessible and remote areas, where it fills in many of the gaps, such as in coastal and polar regions, left by other measurement techniques. In under a decade of having operational status, airborne gravimetry has met most medium resolution requirements, and has the potential to meet the highest. As airborne gravimetry matures as a technology, the major challenge remaining is to improve the accuracy and resolution of the measured gravity field.

Airborne gravimetry combines two measurement systems to estimate the gravity field. Total acceleration of the aircraft is measured by a gravimeter, or an Inertial Navigation System (INS). Accelerations due to the movement of the aircraft are measured with signals from the Global Positioning System (GPS). The difference of these two acceleration measurements is the effect of the gravity field. As the aircraft travels, a time series of georeferenced gravity estimates results. Lower flight speeds lead to higher resolution gravity field estimates. Herein, resolution is defined as the minimum recoverable half wavelength. To minimize attenuation of the gravity signal, flight heights are kept low as well. Figure 1.1 illustrates the basic concept of airborne gravimetry.

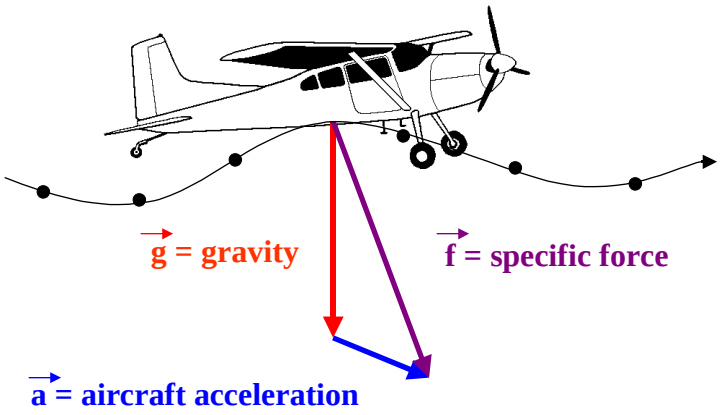

Figure 1.1 Illustration of the airborne gravimetry concept

While vector gravimetry is possible (Schwarz et al., 1991), scalar gravimetry is most common. Usually, scalar gravity disturbances are the first quantity derived, according to the following equation in the local-level frame (Schwarz and Wei, 1994):

$$\delta g_u = \dot{v}_u - f_u - \left(\frac{v_e}{R_1 + h} + 2\omega_{ie} \cos\varphi \right) v_e - \frac{v_n^2}{R_2 + h} - \gamma_u \qquad (1.1)$$

where a dot above a variable denotes time differentiation,

δg_u is the gravity disturbance in the upward direction, measured in mGal (10^{-5} m/s^2),

$\dot{v}_u$ is the upward aircraft acceleration computed from Differential GPS (DGPS) techniques,

f_u is the specific force measured by the gravimeter or INS,

v_e, v_n are aircraft velocities in the east and north directions,

R_1, R_2 are the prime vertical and meridian radii of curvature,

ω_{ie} is the rotation rate of the Earth,

h is height above the ellipsoid,

φ is the ellipsoidal latitude, and

γ_u is upward component of normal gravity.

Different airborne gravimetry system concepts exist, and Equation (1.1) is implemented differently in each system type due to different mechanizations to realize the local-level frame and different hardware. The three currently available types are: strapdown, damped two-axis platform, and stable platform. Details of the first two system concepts are given in Schwarz and Li (1996b), while details of the third system concept are in Czompo and Ferguson (1995).

Depending on the application, the gravity disturbances are either used directly, as for instance in geophysical exploration, or they are used to compute a geoid of the area flown. The accuracy and resolution required of the measured gravity field also depends on the application. For local or regional geoid computation at the centimeter level, gravity measurements are required at five kilometer resolution for mountainous areas, and 14 kilometer resolution for flat areas (Schwarz and Li, 1996). The accuracy of these gravity measurements should be approximately 2 mGal (Timmens et al., 2000, Schwarz and Li, 1996a). For coastal oceanography applications, like sea surface topography, a geoid with an accuracy of at least 5 centimeters is required (Timmens et al., 2000).

Geophysical applications often use gravity disturbances or closely related measures like gravity anomalies, free-air anomalies or Bouguer anomalies. In these applications, the measured gravity field indicates density variations within the Earth's crust, due to geological features and geodynamical processes. The required accuracies and resolutions for studying various geophysical features and applications are given in Figure 1.2 (NRC, 1995, Hein, 1995, Johnson, 1998).

Today's airborne gravimeter systems are capable of meeting many of these requirements. To name a few examples, airborne gravimetry has been successfully used for local and regional geological studies and sub-ice topography (Bell et al., 1999), coastal oceanography (Forsberg et al, 2000), and some exploration geophysics applications (Salychev and Schwarz, 1995, Ferguson and Hammada, 2000). Although the accuracy of

these systems varies, the most accurate are currently able to measure gravity with a standard deviation of between 0.5 and 1.5 mGal at a spatial resolution of about 2 km (half wavelength).

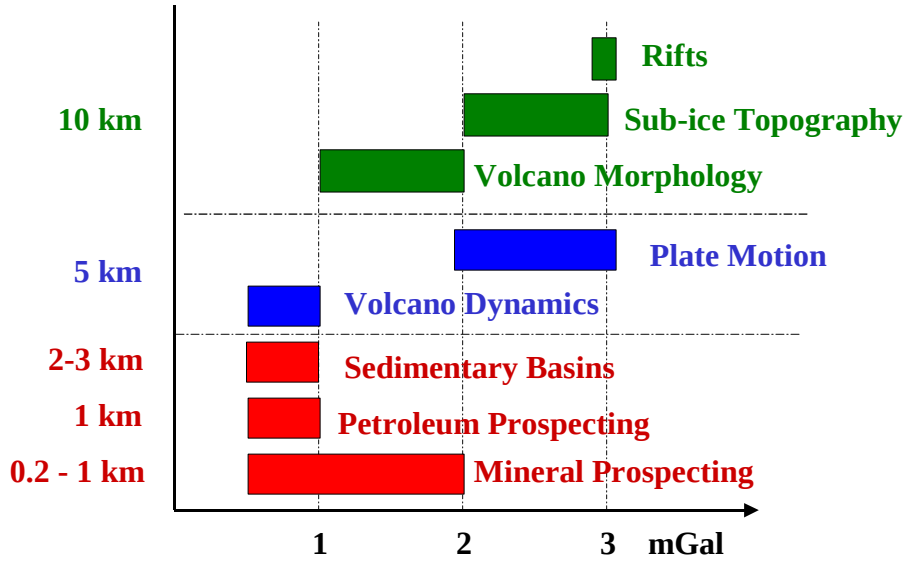

Figure 1.2 Gravity accuracy and resolution requirements for geophysical applications: accuracy in mGal is denoted on the horizontal axis, with resolution on the vertical

The common resolution limiting factor is the quality of aircraft acceleration estimates. Errors in the DGPS accelerations used for motion compensation are one of the main obstacles to achieving greater accuracy at higher resolutions. While INS errors also contribute to the overall error of the gravity estimates, the DGPS acceleration errors are dominant, especially at higher frequencies. Bruton (2000) investigated the effect of DGPS errors on a strapdown airborne gravimetry system. Figure 1.3, taken from Bruton (2000), shows the error spectra of gravity estimates from a morning and an afternoon flight, along with the error spectra of the INS errors.

Figure 1.3 highlights how critical good quality DGPS accelerations are to the results of airborne gravimetry, and how much larger the GPS errors are relative to the INS errors.

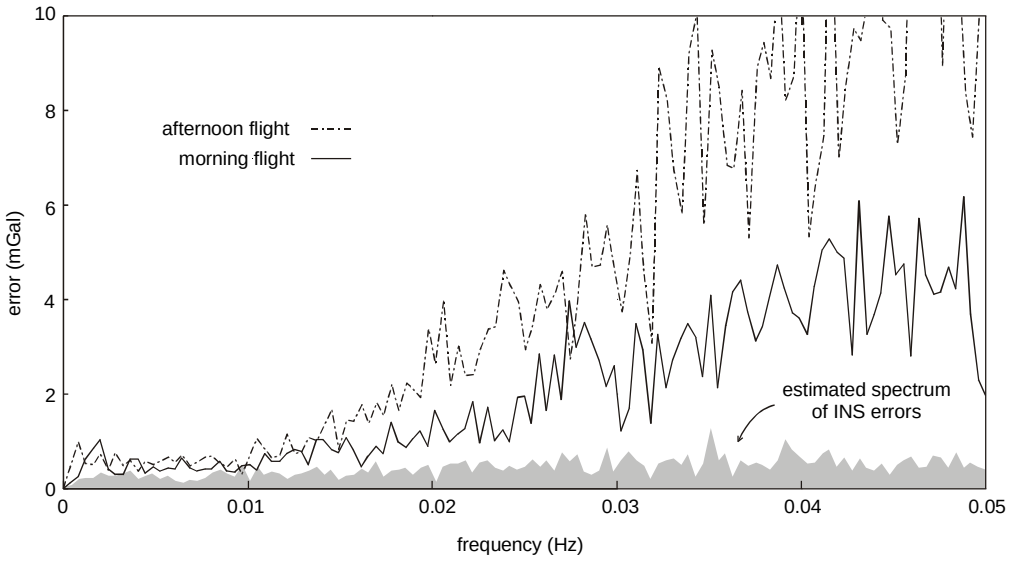

Figure 1.3 Error spectra of two estimates of the gravity field and INS errors, from Bruton (2000)

The comparison of the morning and afternoon flights shows the latter has increased error in the gravity estimates. Ionospheric activity typically has a diurnal maximum in mid-afternoon. This increased ionospheric activity degrades the received GPS signals, and the corresponding accelerations estimated from GPS, leading to the higher level of error in the gravity estimates from the afternoon flight.

When GPS first became operational in the late 1980s and early 1990s, its applicability to airborne gravimetry was immediately recognized. The content of this thesis assumes a thorough understanding of GPS concepts. The reader who is unfamiliar with GPS is referred to Parkinson and Spilker (1996) for a comprehensive GPS reference. The accuracy of accelerations derived from GPS was analyzed by Brozena et al. (1989), Kleusberg (1990), Wei et al. (1991), Czompo (1993), and Van Dierendonck et al. (1994). For these studies the desired resolution limit ranged from 2 to 10 km. The most optimistic result was 0.5 mGal at a 120 s filtering period, achieved with static data (Kleusberg, 1990). However, this is not realistic because the motion error is considered as zero. Using airborne data, and radar as a reference, Brozena et al. (1989) found GPS vertical accelerations to be accurate to 2 mGal over 20km. Also with airborne data, and laser altimetry as a reference, vertical accelerations of 1.5 mGal at 10 km, 4 mGal at 5 km (Czompo, 1993) and 1.5 mGal at 2 km resolution (Van Dierendonck, 1994) were

achieved. Wei et al. (1991) reported GPS acceleration accuracy to be 1 mGal at 3 km resolution. In this study, a reference trajectory, with height standard deviations of maximum 1.5 cm, was provided by a vertical motion machine. In all cases, the authors concluded that accelerations derived from GPS had low error at low frequencies and that errors increased sharply as frequency increased. Each of these studies clearly states that low pass filtering is necessary to produce acceptable vertical accelerations for airborne gravimetry.

Recently, the focus of airborne gravimetry has shifted to high resolution applications in geophysical prospecting and exploration. An often-quoted requirement is 1 mGal accuracy at 1 km resolution (NRC, 1995). From this perspective, low pass filtering is not a viable means of removing high frequency noise from the vertical accelerations, as it also limits the resolution of the recovered gravity field. Since previous investigations have focused on half-wavelengths above 3 km, the question remains as to whether GPS can provide accelerations of higher accuracy at higher frequencies. Schwarz and Li (1996a) identified improving GPS kinematic accelerations as a critical factor to improving the performance of airborne gravimetry in the high frequency part of the spectrum.

Improvements in vertical accelerations would benefit all three types of currently available airborne gravimetry systems: strapdown, damped two-axis platform, and stable platform. Bell et al. (1999) employed a damped two-axis platform system and cited GPS accelerations as limiting the accuracy of airborne gravimetry. With respect to results from an inertial platform system, Bruton et al. (2001a) reports the current quality of vertical aircraft accelerations is curbing the potential of the system for very short wavelength recovery. Since strapdown gravimeters do not have hardware imposed filtering, their potential for providing high resolution data is very good. However, they are especially hampered by the quality of vertical accelerations derived from GPS, as it is their main limiting factor (Bruton, 2000).

The preferred method of deriving acceleration from GPS is to twice time differentiate GPS positions. This method will be referred to as the position method. Exceptions are Kleusberg (1990), Peyton (1990), and Jekeli and Garcia (1997). For 1 mGal accuracy, GPS positions at the meter level are required for the computation of normal gravity, and GPS velocities at the cm/s level are needed to calculate the Eötvös correction. However, to achieve 1 mGal accuracy in accelerations estimated by differentiating GPS positions, those positions must be accurate to the centimeter level (Wei et al., 1991), if a 60 s filter is applied. Kinematic positioning at the centimeter level in an airborne environment is achievable only under optimal conditions, and with careful processing.

Aircraft accelerations are computed from the position trajectory by numerical differentiation. Consideration must be given to the spectral properties of both the positions and the differentiator. Essentially, the task of differentiating the DPGS positions is a discrete time signal processing problem and the chosen filter should not be chosen blindly. In Bruton et al. (1999) the performance of various differentiating filter designs were examined with respect to their frequency responses, and the frequency content of the signals they were applied to. It was concluded that differentiator bandwidth should match the bandwidth of the signal to produce the best estimation of the derivative. Current results give the accuracy of accelerations derived from GPS positions to be 1.5 mGal at 2 km and 2.5 mGal at 1.4 km resolution when appropriate GPS processing and differentiators are applied (Bruton, 2000).

Appropriate GPS processing for precise acceleration determination via the position method requires meticulous care, beyond standard procedures for precise position processing. If a discontinuity exists in the position trajectory, the velocity and acceleration estimates resulting from differentiating the positions will be corrupted by edge effects. Discontinuities due to aircraft motion are not expected during a typical airborne gravimetry flight. Aircraft velocity and height are kept very close to constant. However, sudden jumps in the position trajectory can be caused by incorrect ambiguity fixes, and the gain or loss of a satellite (Bell et al., 1999, Brozena and Childers, 2000, Bruton, 2000). Changes in the positional variance, resulting from the inclusion of a low

elevation satellite or switching between float and fixed ambiguity mode, can also cause edge effects in the estimated accelerations. Thus, the user must carefully process the DGPS positions. This usually entails processing flights lines forwards and backwards in time and comparing the position trajectories to detect errors resulting from satellite introduction or elimination. The satellite set used must be monitored and often controlled, increasing the amount of user input and disregarding available satellites.

Since the position method of estimating accelerations is not meeting the accuracy requirements necessary at higher frequencies and requires intensively monitored processing, other options need to be explored. Kleusberg (1990), Peyton (1990), Jekeli (1994) and Jekeli and Garcia (1997) proposed estimating accelerations directly from carrier phase measurements. The benefits of this approach are: very precise positions are no longer required, algorithmic advantages to cope with less than optimal data collection conditions, and a solution optimized in the acceleration domain. A minimization of errors in the position domain may not necessarily remain optimal once it is differentiated into the acceleration domain. Operational results with this type of algorithm, and comparison with the position method, were first presented in Kennedy et al. (2001). They show preliminary promise of being better suited to acceleration estimation in airborne gravimetry.

1.1 Statement of Problem

As a mature technology, airborne gravimetry needs to be refined in order to meet the stringent requirements of some geophysical applications. While DGPS made operational airborne gravimetry possible in the early to mid 1990s, it has emerged as a main limiting factor in achievable accuracy and resolution. The question arises if current processing methods optimally derive acceleration from GPS measurements. The standard method of estimating accelerations from GPS is to twice time differentiate aircraft positions. This method is convenient as aircraft positions are already required for gravity disturbance estimation.

However, it has been shown to be insufficient for very high resolution applications, even when processed as carefully as possible. GPS positioning packages are optimized in the position domain, but optimality in the acceleration domain is both defined and achieved differently. In terms of positioning, biases are not considered tolerable; whereas, small jumps in position may be. When differentiating into the acceleration domain, the reverse is true. A constantly biased, but smooth, estimated trajectory is perfectly acceptable when estimating acceleration with the position method. Therefore, alternative processing schemes need to be investigated, to determine if there is another way to derive aircraft accelerations from GPS that is more suited to airborne gravimetry.

One such alternative estimates accelerations directly from carrier phase measurements, which will be referred to as the carrier method herein. This allows for errors to be minimized in the acceleration domain. It can also provide control over which satellites are used and how they are used in the acceleration solution. In addition, position accuracy requirements are the same as they are for normal gravity calculation, on the order of meters, which relaxes the need for very precise positions, simplifying the GPS processing required.

1.2 Research Objectives

The objective of this research is to develop and evaluate an alternative processing scheme for deriving accelerations from GPS. This alternative processing scheme estimates accelerations directly from carrier phase measurements. The results obtained with the alternative processing scheme will be compared to the position method results, with both methods using agreement to an independent reference gravity field to quantify their accuracy. The aim is to answer the following questions:

1. Does estimating accelerations directly from carrier phase measurements provide any improvement in the accuracy of vertical accelerations required for airborne gravimetry, over the full range of conditions encountered in practice?

2. Does this method provide any algorithmic advantages specifically for airborne gravimetry, making it comparatively superior in implementation?

Since the goal is a direct comparison of the position and carrier phase methods of determining accelerations from GPS, both methods must be tested under identical conditions, representative of an operational airborne gravimetry campaign. To satisfy these requirements, the same datasets are used for computations with both methods. The criterion for evaluation is agreement with a reference field. Two sets of gravity disturbances are computed: one using aircraft accelerations from the position method and the other using aircraft accelerations from the carrier phase method. The same specific force measurements are used in both gravity disturbance estimates.

Data from an airborne gravimetry campaign flown over the Alexandria area (near Ottawa, Canada) in the spring of 2000 is used. This campaign has several days of flying, under varying conditions, with repeat passes of the same lines. A reference gravity field is available for the area as well, computed from ground measurements and upward continued to flight level.

The algorithm for estimating accelerations from carrier phase measurements presented in Jekeli and Garcia (1997) is used as the base for the processing scheme developed. This original carrier phase method is modified to create a more robust and sophisticated algorithm, which uses all available satellite measurements. The original carrier phase method is a unique acceleration solution, restricting the user to measurements from only four satellites.

The modified carrier phase method incorporates a least squares solution with a full covariance model, allowing for the use of all available satellites and weighting their contribution to the solution. The covariance model has been specifically developed for carrier phase measurements and their derivatives and is an expansion of the model presented in Radovanovic et al. (2001). It models ionospheric and tropospheric variances. Physical and mathematical correlations are taken into account, resulting in the

use of a fully populated covariance matrix in the solution. The modified carrier phase method is compared to the original carrier phase method, to show that the modifications improve performance.

Following this, the modified carrier phase method is compared to the position method. Differences in performance are analyzed under varying conditions. Each method's response to low quality positions, low satellite availability, high ionospheric conditions, and satellite constellation changes is evaluated. These different scenarios are representative of conditions that would be encountered in an operational flight.

Based on analysis and interpretation of the results from the above comparisons, a summary of the strengths and limitations of the modified carrier phase method is presented. Conclusions as to whether or not it is superior to the position method, in terms of accuracy and algorithmic or operational advantages, are made in response to the questions posed as the research objectives.

Chapter 2

Acceleration Estimation in Airborne Gravimetry

Aircraft accelerations are required in airborne gravimetry for motion compensation. The accuracy of the accelerations, derived from GPS, is key to the accuracy of the estimated gravity field. As cited in Section 1.0, the currently achieved accuracy of GPS accelerations is limiting the resolution of airborne gravimetry systems and thus their use in high resolution applications. This problem is common to all three types of airborne gravimetry systems currently available: strapdown, 2-axis damped, and stable platform. Although there are differences in the methodology and hardware of each system type, the common major obstacle impeding their use for very high resolution work (e.g. below 3 km) is errors in the DGPS accelerations. For recent results obtained with these system concepts, see Ferguson and Hammada (2000), Bruton et al. (2001a), and Williams and MacQueen (2001). In scalar gravimetry, the effect of errors in the upward aircraft accelerations is the same for each system, which can be seen by reviewing the error models for each system.

The error model for strapdown scalar gravimetry is given in Schwarz and Wei (1994), Schwarz and Li (1996b), and Glennie (1999). For the damped 2-axis approach, used in the LaCoste Romberg (LCR) systems, the error model is given in Olesen et al. (1997) and Glennie et al. (2000). For the stable platform gravimetry, the error model is given in Czompo and Ferguson (1995). The basic error model equation for an airborne gravimetry system can be summarized as follows:

$$d\delta g = -d\dot{v}_u + d_{specific\_force} + d_{misalignment} + d_{time} \tag{2.1}$$

where $d\delta g$ is the error of the estimated gravity disturbance,

$d\dot{v}_u$ is the DGPS aircraft acceleration error in the upward direction,

$d_{specific\_force}$ represents the errors due to errors in the specific force measurements,

$d_{misalignment}$ represents the error due to misalignment (including gyro drift), and

d_{time} is the error caused by the time synchronization error between the INS and GPS data streams.

The form of the specific force and misalignment errors is slightly different for each system type, due to hardware and mechanization differences. However, the effect of upward DGPS acceleration errors is the same for all system types, as can be seen in Equation (2.1). The terms of Equation (2.1) that vary with system type are presented in the following, for completeness.

With a strapdown system, the effect of the specific force measurement errors on the estimated gravity disturbance is given as:

$$d_{specific\_force} = \begin{bmatrix} -\cos\theta\sin\phi & \sin\theta & \cos\theta\cos\phi \end{bmatrix} \begin{bmatrix} df_x^b \\ df_y^b \\ df_z^b \end{bmatrix} \tag{2.2a}$$

where θ, ϕ are the pitch and roll angles of the body to local level frame transformation and

df_x^b, df_y^b, df_z^b are the specific force errors in the body frame.

In a strapdown system, alignment with the local level frame is achieved computationally, rather than realized physically. This alignment is not perfect, resulting in a misalignment error that is conceptually similar to a tilt error in a stable platform system. The misalignment error is due to horizontal acceleration errors, as well as specific force measurement errors. For scalar airborne gravimetry, misalignments about the north and east axes are of concern, while a misalignment about the up axis does not have an effect. The error in the estimated gravity disturbance due to the misalignment of the strapdown airborne gravimeter is given as:

$$d_{misalignment} = \varepsilon_N f_e - \varepsilon_E f_n \tag{2.2b}$$

where $\varepsilon_N, \varepsilon_E$ are the misalignments about the north and east directions and

f_e, f_n are the specific force measurements in the east and north directions.

With the damped 2-axis approach, the local level frame is physically approximated by the system platform. The horizontal and vertical specific force errors are considered somewhat separately, as the horizontal specific force errors contribute to the misalignment error. With respect to the gravity disturbance estimated in the local level frame, the specific force error for the damped 2-axis approach is:

$$d_{specific\_force} = df_u \tag{2.3a}$$

where df_u is the upward specific force error.

The damped 2-axis system has another error term, which is particular to this system type and the manner in which the local level approximation is physically realized. There is a cross coupling correction applied to the upward specific force measurement in the gravity disturbance estimation with the damped 2-axis system. Hence, the error in this cross coupling correction should be included in the specific force error given in Equation (2.3a). To highlight the similarities between the system types, the cross coupling correction error is shown separately in Equation (2.3b) below.

$$\begin{aligned} d_{cross\_coupling} &= (a_3 v_b + 2 f_x a_5 v_b) df_x + (a_2 p_b + a_4 v_b) df_y \\ &\quad (2 a_1 v_b + a_3 f_x + a_4 f_y + a_5 f_x^{\,2}) dv_b + (a_2 f_y) dp_b \\ &\quad (v_b^{\,2}) da_1 + (f_y p_b) da_2 + (f_x v_b) da_3 + (f_y v_b) da_4 + (f_x^{\,2} v_b) da_5 \end{aligned} \tag{2.3b}$$

where f_x, f_y are the cross-track and along-track specific force measurements,

df_x, df_y are the errors in those measurements,

v_b, dv_b are the beam velocity and its error,

p_b, dp_b are the beam position and its error, and

$a_1 ... a_5, da_1 ... da_5$ are statistically or empirically derived coefficients, and their errors.

The cross coupling correction does not appear in the error models for strapdown or stable platform systems. In a strapdown system, it is taken care of computationally, as the local level frame is not realized physically. In a stable platform system, the cross coupling correction is mechanically approximated and the platform is very closely aligned to the local level frame.

The error caused by misalignment for the damped 2-axis system is given as:

$$d_{misalignment} = \frac{f_x}{g}\ df_x + \frac{f_y}{g}\ df_y - \frac{\dot{v}_E}{g}\ d\dot{v}_E - \frac{\dot{v}_N}{g}\ d\dot{v}_N \tag{2.3c}$$

where g is the magnitude of gravity

$\dot{v}_e, \dot{v}_n$ are the DGPS aircraft accelerations in the east and north directions, and

$d\dot{v}_e, d\dot{v}_n$ are the errors in those aircraft accelerations, and

all other terms are as defined previously.

Lastly, the stable platform system has specific force and misalignment errors very similar to the damped 2-axis platform, as it also approximates the local level frame, but much more accurately. The upward accelerometer can be expected to be aligned to within one arc minute, or better, of the gravity vector which is why the upward specific force measurement is used in the misalignment error term, rather than the magnitude of gravity. (In the damped 2-axis system, the upward accelerometer may be misaligned with the gravity vector by up to one degree.) The error in the estimated gravity disturbance due to specific force errors in the stable platform system is:

$$d_{specific\_force} = df_u \tag{2.4a}$$

where df_u is the error in the upward specific force measurement, as before.

The misalignment error for the stable platform system is:

$$d_{misalignment} = \frac{f_x}{f_u}\ df_x + \frac{f_y}{f_u}\ df_y - \frac{\dot{v}_E}{f_u}\ d\dot{v}_E - \frac{\dot{v}_N}{f_u}\ d\dot{v}_N \qquad (2.4b)$$

where all terms are as defined previously.

Since the effect of the DGPS acceleration errors is identical in all systems, improvements in the DGPS accelerations will benefit all systems. Especially in the 2-axis damped platform systems, the benefit will be limited by any low pass filtering inherent in the hardware. Research is being conducted to attempt to reduce the amount of low pass filtering (Childers, 1999), but a significant amount is still required, which limits the resolution of the 2-axis damped platform systems. In these systems, improvements in the DGPS accelerations above the cut-off frequency of the low pass filtering will not be of benefit. However, with strapdown gravimeters there is no low pass filtering imposed by the hardware. If the level of low pass filtering required to remove noise from the DGPS accelerations can be reduced, the high frequency performance of strapdown systems will be dramatically improved.

As the current method of obtaining DGPS accelerations does not provide the desired accuracy and has operational constraints, alternative methods must be investigated. The current method of differentiating positions is reviewed in Section 2.1. The basic methodology of estimating accelerations directly from carrier phases is presented in Section 2.2, and extended in Chapter 3 to form the modified carrier method.

2.1 The Position Method of Acceleration Estimation

The most widely accepted method of determining aircraft accelerations from DGPS is to twice time-differentiate the aircraft trajectory. Many issues surrounding the position method are examined in Bruton (2000), to which the reader is referred for a comprehensive reference. The position method is convenient as positions are already required for the normal gravity calculation. The differentiation is usually performed by applying a differentiating filter in cascade, as velocities are also required for the Eötvös correction. DGPS positioning accuracy and differentiator selection determine the accuracy and bandwidth of the estimated accelerations. This relationship is defined in Wei et al. (1991), and quantified by the following equation:

$$\sigma_a = \frac{4\pi^2}{\sqrt{5}} f_c^{5/2} \sigma_h \tag{2.1.1}$$

where σ_a, σ_h are the standard deviations of the acceleration and height errors, respectively, and

f_c is the cut-off frequency of whatever filter has been applied to the heights.

The cut-off frequency in Equation 2.1.1 is the extent of the effective bandwidth of the chosen differentiator, or the cut-off frequency of an applied low pass filter. Realizable differentiators, of the type normally applied in airborne gravimetry, have a cut-off frequency. They only approximate the ideal differentiator over a specific bandwidth, and behave similarly to a low pass filter beyond their bandwidth. The quality of the estimated derivative is very dependent on the chosen differentiator, as shown in Cannon et al. (1997), Ryan et al. (1997), and Bruton et al. 1999). As concluded in Bruton (2000), the differentiator bandwidth should match the frequency range of the dynamics of the aircraft. Further discussion of differentiators is left to Section 3.1.

The other, and most important, factor in the accuracy of accelerations is the accuracy of the positions used to estimate them. Using Equation (2.1.1), with a cut-off frequency

equivalent to 1.4 km resolution (flight speed of 45 m/s), the position accuracy must be at the centimeter level for sub-mGal acceleration accuracy. With the current GPS constellation and operational conditions in airborne gravimetry, reliably positioning at the centimeter level in height is not possible. This was well illustrated in a recent comparison of commercial GPS processing packages in Bruton et al. (2001b) that showed meter level differences on the same kinematic data set. Baselines in airborne gravimetry are rarely less than 50 km and often are hundreds of kilometers long, due to the typically large and remote areas covered. Additionally, timing of flights cannot always be planned to avoid diurnal highs in ionospheric activity. Under these conditions, only decimeter level positioning can be realistically expected. Improvements in positioning accuracy are expected with the planned modernization of GPS. This will certainly help, but the modernized system is not projected to be fully available until approximately 2012 (Shaw et al., 2000).

GPS processing in airborne gravimetry is not a blind process. Changes in the visible constellation often produce jumps in the position trajectory (Bell et al., 1999, Bruton, 2000, Brozena and Childers, 2000). While not posing a problem in the position domain, these small discontinuities translate into large acceleration errors once differentiated. The inclusion of low elevation satellites can also degrade the position solution, which also produces acceleration errors (Bruton, 2000). To achieve optimal results, for airborne gravimetry, the satellite constellation used in the position solution must be carefully controlled, to avoid the loss or gain of satellites while on the same flight line and to cautiously use low elevation satellites. This can result in using far fewer satellites than available, which is also not ideal.

Also of concern is ambiguity fixing. Reliably fixing ambiguities is difficult over long baselines, but if possible the L1 fixed solution provides the best results for airborne gravimetry (Bruton, 2000). The danger lies in an incorrect set of ambiguities being fixed, and then reset once residual testing shows the set to be in error. The reset can lead to discontinuities in the position solution, which will corrupt the acceleration solution.

Using the ionospheric free solution is often necessary, and avoids the problem of sudden changes in the ambiguities, but also increases the noise level, thus lowering the accuracy.

In summary, the position method hinges on excellent positioning accuracy, which may not be consistently acheivable under operational conditions. The accuracy of DGPS accelerations derived in this manner is the main limiting factor of airborne gravimetry.

2.2 The Carrier Method of Acceleration Estimation

An alternative to the position method of estimating accelerations from GPS is to estimate accelerations directly from the carrier phase measurements, and their derivatives. This method was proposed by Kleusberg et al. (1990), Peyton (1990), and Jekeli (1994). Kleusberg et al. (1990) and Peyton (1990) presented only static results in the acceleration domain. The work in Jekeli (1994) was continued in Jekeli and Garcia (1997), with kinematic acceleration results presented. Preliminary, promising results in the gravity domain were first presented in Kennedy et al. (2001). The most extensive testing and evaluation of the method to date is presented in this thesis. One of the main advantages of the carrier method is positioning accuracy can be relaxed to the order of meters.

The algorithm of the carrier method presented in this section can be found in Jekeli and Garcia (1997). While all the equations presented in this section stem from that source, they are presented here in a different manner for clarity. Additional commentary is also provided herein, to allow for better comprehension of the implementation of the carrier method.

2.2.1 Review of the Carrier Phase Observable

Basically, the acceleration of a GPS antenna can be determined by differentiating carrier phase measurements with respect to time to determine line of sight range rates and range accelerations. It is useful to review the carrier phase observable, to examine the error sources and the effect differentiation has on them. The carrier phase observable between satellite ‘p’ and receiver antenna ‘m’, in meters, is given as:

$$\phi_m^p = \rho_m^p + d\rho + c(dt^p - dT_m) + \lambda N - d_{ion} + d_{trop} + d_{multi} + \varepsilon_\phi \quad (2.2.1)$$

where ρ_m^p is the geometric range between satellite 'p' and receiver antenna 'm',

$d\rho$ is the orbital error,

c is the speed of light in m/s,

dt^p is the satellite clock error in seconds,

dT_m is the receiver clock error in seconds,

λN is wavelength multiplied by the ambiguity,

d_{ion} is the ionospheric error,

d_{trop} is the tropospheric error,

d_{multi} is the multipath error, and

ε_ϕ is the noise.

A thorough review of the behavior and magnitude of each error source can be found in Racquet (1998) or Bruton (2000). The latter considers the errors sources and their effects in the context of airborne gravimetry specifically.

Differentiating the carrier phase observable gives line of sight velocity and, if performed a second time, acceleration. This has some advantageous effects. Namely, all constant terms will be removed in both the first and second carrier phase derivatives; therefore, the ambiguity term vanishes. The second derivative will also have all first-order terms removed, which will reduce all error sources. This is potentially useful when one bears in mind that the L1/L2 ionospheric free combination can also only remove first order effects of the ionosphere. With the assumption that higher order orbital errors, ionospheric and tropospheric errors, and the multipath error are absorbed into the noise term, the first and second carrier phase derivatives are as follows:

$$\dot{\phi}_m^p = \dot{\rho}_m^p + c(\dot{dt}^p - \dot{dT}_m) + \varepsilon_{\dot{\phi}} \quad (2.2.2)$$

$$\ddot{\phi}_m^p = \ddot{\rho}_m^p + c(\ddot{dt}^p - \ddot{dT}_m) + \varepsilon_{\ddot{\phi}} \tag{2.2.3}$$

where the terms are as defined before, with the superscript dots indicating time differentiation.

The remaining clock terms can be eliminated by double differencing, which will further reduce the ionospheric and tropospheric terms. In this way the carrier phase derivatives approximate the range rate and range acceleration between the satellite and receiver antenna, as the following approximation holds:

$$\phi_{m,k}^{p,q} \cong \rho_{m,k}^{p,q} \ . \tag{2.2.4}$$

At this point it should be noted that while differentiation has benefits in reducing some error sources, differentiation demands careful cycle slip detection. Cycle slips must be corrected or large edge effects will result from the differentiating filter passing over the discontinuity in the carrier phase measurements. Figure 2.2.1 illustrates edge effects created by a differentiating filter comprised of five samples applied to data simulating carrier phase measurements with a cycle slip. Issues surrounding the differentiation process will be discussed in Section 3.1.

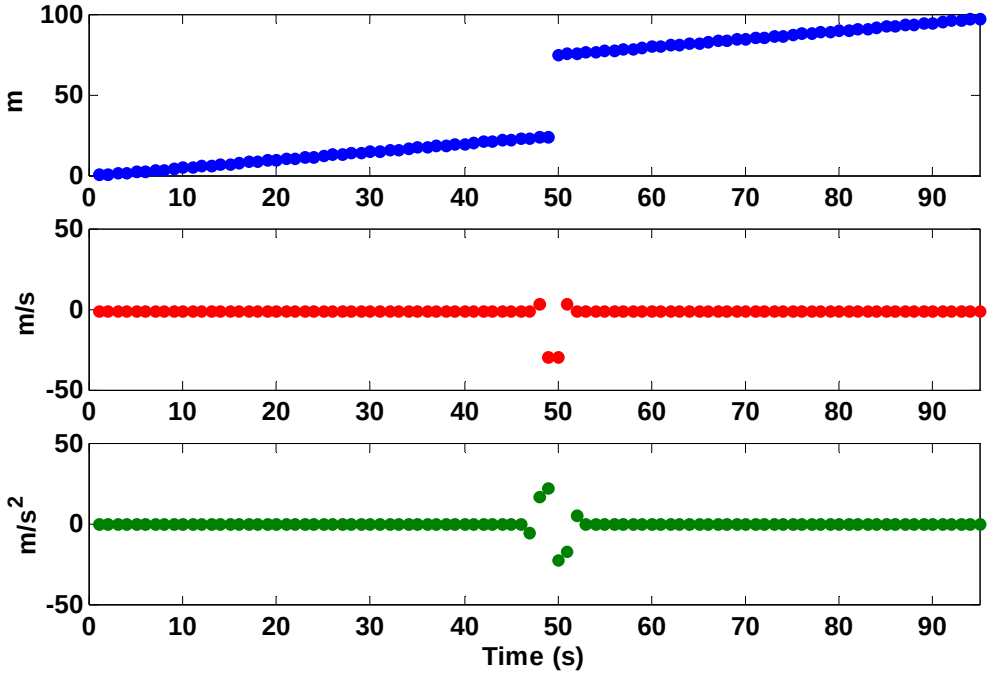

Figure 2.2.1 Edge effects caused by applying a differentiator of length 5 to data simulating carrier phases with a cycle slip

2.2.2 Fundamental Equations of the Carrier Method

In the following, satellites are indicated in the superscript and receivers in the subscript. The base receiver is indicated as receiver ‘k’, while the rover is receiver ‘m’. Bolded quantities indicate vectors or matrices. Superscript dots indicate time differentiation.

In Section 2.2.1, it has been shown that measurements of the range rate and acceleration can be obtained, allowing the carrier method to be derived. Since it is a relative process, the following equations can be realized in any frame that is convenient, provided the proper corrections are applied to the final acceleration solution if it is transformed into another frame (Schwarz and Wei, 2000). The carrier method is based on the geometric relationship shown in Figure 2.2.2 and given in Equation (2.2.5).

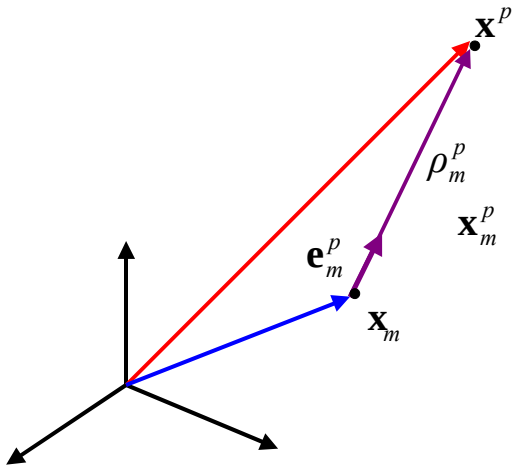

Figure 2.2.2 Relative geometry between receiver 'm' and satellite 'p'

$$\mathbf{x}_m^p = \rho_m^p \mathbf{e}_m^p \tag{2.2.5}$$

where $\mathbf{x}_m^p$ is the relative position vector between receiver antenna 'm' and satellite 'p'

ρ_m^p is the geometric range between receiver antenna 'm' and satellite 'p'

$\mathbf{e}_m^p$ is the unit direction vector from receiver antenna 'm' to satellite 'p'

If Equation (2.2.5) is differentiated, it becomes:

$$\dot{\mathbf{x}}_m^p = \dot{\rho}_m^p \mathbf{e}_m^p + \rho_m^p \dot{\mathbf{e}}_m^p \tag{2.2.6}$$

which will be useful in further derivations. Closely related to Equation (2.2.5) is:

$$\rho_m^p = \mathbf{e}_m^p \cdot \mathbf{x}_m^p \tag{2.2.7}$$

This is the fundamental equation of the carrier method. The geometric range between satellite 'p' and receiver 'm' establishes the line-of-sight relationship. Once differentiated, it gives the line-of-sight range rate, which is analogous to the Doppler measurement from the receiver or can be derived by differentiating the carrier phases.

$$\dot{\rho}_m^p = \dot{\mathbf{e}}_m^p \cdot \mathbf{x}_m^p + \mathbf{e}_m^p \cdot \dot{\mathbf{x}}_m^p \tag{2.2.8a}$$

The first term on the right side of Equation (2.2.8a) is zero. Recalling Equation (2.2.5) and that the derivative of a vector lies perpendicular to it, the inner product of the first term is zero, as $\dot{\mathbf{e}}_m^p$ and $\mathbf{x}_m^p$ are normal to each other. Equation (2.2.8a) becomes:

$$\dot{\rho}_m^p = \mathbf{e}_m^p \cdot \dot{\mathbf{x}}_m^p \tag{2.2.8}$$

Differentiating once more gives the acceleration between the receiver and the satellite.

$$\ddot{\rho}_m^p = \mathbf{e}_m^p \cdot \ddot{\mathbf{x}}_m^p + \dot{\mathbf{e}}_m^p \cdot \dot{\mathbf{x}}_m^p \tag{2.2.9}$$

This range acceleration resembles the curvilinear acceleration equation where the total acceleration is the sum of the acceleration normal and tangent to the path of travel. Figure 2.2.3 shows this graphically.

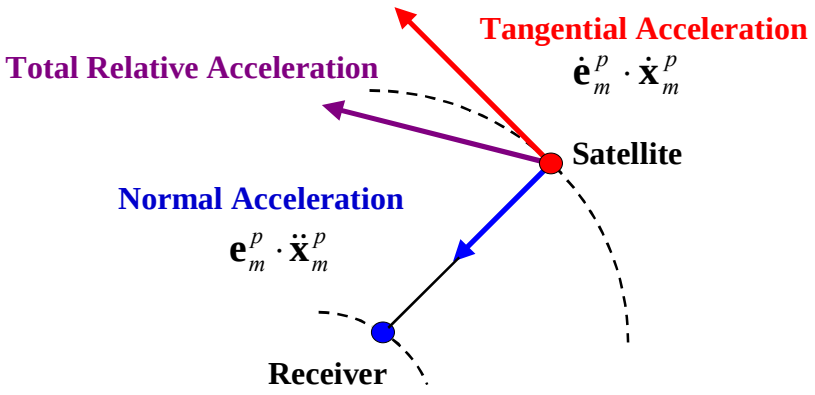

Figure 2.2.3 Relative receiver-satellite acceleration

The solution of Equation (2.2.9) for receiver acceleration requires an expression for $\dot{\mathbf{e}}_m^p$ in terms that are known for easy computation. This expression can be found by rearranging (2.2.6) to give:

$$\dot{\mathbf{e}}_m^p = \frac{1}{\rho_m^p}\dot{\mathbf{x}}_m^p - \frac{1}{\rho_m^p}\dot{\rho}_m^p \mathbf{e}_m^p \tag{2.2.10}$$

Then, forming the dot product of $\dot{\mathbf{e}}_m^p$ and $\dot{\mathbf{x}}_m^p$, the second term on the right of Equation (2.2.9), is:

$$\dot{\mathbf{e}}_m^p \cdot \dot{\mathbf{x}}_m^p = \frac{1}{\rho_m^p}\dot{\mathbf{x}}_m^p \cdot \dot{\mathbf{x}}_m^p - \frac{\dot{\rho}_m^p}{\rho_m^p}\mathbf{e}_m^p \cdot \dot{\mathbf{x}}_m^p \tag{2.2.11a}$$

Substituting in Equation (2.2.6) for $\dot{\mathbf{x}}_m^p$ gives:

$$\dot{\mathbf{e}}_m^p \cdot \dot{\mathbf{x}}_m^p = \frac{1}{\rho_m^p}\left|\dot{\mathbf{x}}_m^p\right|^2 - \frac{\dot{\rho}_m^p}{\rho_m^p}\mathbf{e}_m^p \cdot (\dot{\rho}_m^p \mathbf{e}_m^p + \rho_m^p \dot{\mathbf{e}}_m^p) \tag{2.2.11b}$$

Moving the scalar $\dot{\rho}_m^p$ through the brackets, recalling that $\dot{\mathbf{e}}_m^p$ and $\mathbf{e}_m^p$ are normal to each other, and that $\mathbf{e}_m^p$ is a unit vector, such that $\mathbf{e}_m^p \cdot \mathbf{e}_m^p = \left|\mathbf{e}_m^p\right|^2 = 1$, this reduces to:

$$\dot{\mathbf{e}}_m^p \cdot \dot{\mathbf{x}}_m^p = \frac{1}{\rho_m^p}\left[\left|\dot{\mathbf{x}}_m^p\right|^2 - (\dot{\rho}_m^p)^2\right] \tag{2.2.11}$$

Using Equation (2.2.11) and vector subtraction to separate $\ddot{\mathbf{x}}_m^p$, Equation (2.2.9) can be written as:

$$\ddot{\rho}_m^p = \mathbf{e}_m^p \cdot (\ddot{\mathbf{x}}^p - \ddot{\mathbf{x}}_m) + \frac{1}{\rho_m^p}\left[\left|\dot{\mathbf{x}}_m^p\right|^2 - (\dot{\rho}_m^p)^2\right] \tag{2.2.12}$$

The remaining unknown, besides receiver acceleration, in Equation (2.2.12) is the relative receiver-satellite velocity $\dot{\mathbf{x}}_m^p$. It is solved for using Equation (2.2.8) and is the first step towards the acceleration solution presented in Section 2.2.3.

2.2.3 Model for Acceleration Estimation by the Carrier Method

The original carrier method utilizes measurements from four satellites, resulting in a unique solution for the receiver acceleration, as differencing is employed. The satellites are denoted by 'p', 'q', 'r', and 's', the remote receiver by 'm', and the base receiver by 'k'. In addition the carrier phase derivatives, satellite positions, velocities and accelerations must be known, as well as the receiver antenna positions. Details on how to obtain these quantities are given in Section 3.4.

The goal is to solve Equation (2.2.12) for $\ddot{\mathbf{x}}_m$. Before this can be done the relative receiver-satellite velocity term must be solved for. Equation (2.2.8) is between-satellite differenced to give:

$$\dot{\rho}_m^{p,q} = \mathbf{e}_m^p \cdot \dot{\mathbf{x}}_m^p - \mathbf{e}_m^q \cdot \dot{\mathbf{x}}_m^q \tag{2.2.13a}$$

To solve for $\dot{\mathbf{x}}_m^p$, three equations are required. In each equation, the relative velocity terms must be put in terms of $\dot{\mathbf{x}}_m^p$. Using the vector addition shown in Figure 2.2.4, this can be done.

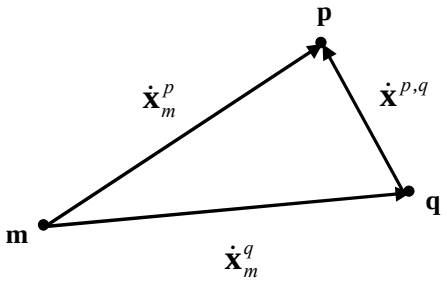

Figure 2.2.4 Relative velocity vectors

Repeating Equation (2.2.13a) for the remaining two satellites, using vector addition to put each in terms of satellite ‘p’, and rearranging to isolate the unknown $\dot{\mathbf{x}}_m^p$ gives:

$$\begin{aligned}
\dot{\rho}_m^{p,q} - \mathbf{e}_m^q \cdot (\dot{\mathbf{x}}^p - \dot{\mathbf{x}}^q) &= (\mathbf{e}_m^p - \mathbf{e}_m^q) \cdot \dot{\mathbf{x}}_m^p \\
\dot{\rho}_m^{p,r} - \mathbf{e}_m^r \cdot (\dot{\mathbf{x}}^p - \dot{\mathbf{x}}^r) &= (\mathbf{e}_m^p - \mathbf{e}_m^r) \cdot \dot{\mathbf{x}}_m^p \\
\dot{\rho}_m^{p,s} - \mathbf{e}_m^s \cdot (\dot{\mathbf{x}}^p - \dot{\mathbf{x}}^s) &= (\mathbf{e}_m^p - \mathbf{e}_m^s) \cdot \dot{\mathbf{x}}_m^p
\end{aligned} \tag{2.2.13}$$

This system of equations can be rewritten as:

$$\mathbf{b} = \mathbf{E}\dot{\mathbf{x}}_m^p \tag{2.2.14}$$

where $\mathbf{E}$ is a matrix with three rows and columns comprised of the transposed, differenced direction vectors in (2.2.13), and $\mathbf{b}$ a matrix with three rows made up of the left hand side of (2.2.13).

Equation (2.2.14) can be solved as:

$$\dot{\mathbf{x}}_m^p = \mathbf{E}^{-1}\mathbf{b} \tag{2.2.15}$$

A solution for all four receiver-satellite velocities must be obtained, using the system of equations in (2.2.13) with each satellite as the base satellite. It must be noted that $\dot{\rho}_m^{p,q}$ is the result of double differencing $\dot{\phi}_m^p$, $\dot{\phi}_m^q$, $\dot{\phi}_k^p$, and $\dot{\phi}_k^q$ (to remove all clock terms and reduce spatially correlated errors), and then adding $\dot{\phi}_k^{p,q}$, computed from Equation (2.2.8) using the knowledge that $\dot{\mathbf{x}}_k^p = \dot{\mathbf{x}}^p$, since $\dot{\mathbf{x}}_k = 0$, as the base station is stationary.

Before moving onto the acceleration solution, it is worthwhile to examine the system of equations in (2.2.13) to evaluate which terms are most critical in determining the

accuracy of the relative velocity solution. As explained in Jekeli (1994) the quality of the satellite and receiver positions is not crucial because they are used to compute direction vectors between the GPS antenna and satellite. Considering that the distance between them is over 20,000 km, even 10 m of positional error is acceptable for sub-mGal accuracies. Errors in the $\dot{\rho}_m^{p,q}$ terms and satellite velocities will have a greater impact on the relative velocity solution.

With all four relative velocities now solved, a system of equations based on Equation (2.2.12) can be formed by single differencing between satellites.

$$
\begin{aligned}
-\ddot{\rho}_m^{p,q} + (\mathbf{e}_m^p \cdot \ddot{\mathbf{x}}^p - \mathbf{e}_m^q \cdot \ddot{\mathbf{x}}^q) + \left(\frac{1}{\rho_m^p}\left[\left|\dot{\mathbf{x}}_m^p\right|^2 - (\dot{\rho}_m^p)^2\right] - \frac{1}{\rho_m^q}\left[\left|\dot{\mathbf{x}}_m^q\right|^2 - (\dot{\rho}_m^q)^2\right]\right) &= \mathbf{e}_m^{p,q} \cdot \ddot{\mathbf{x}}_m \\
-\ddot{\rho}_m^{q,r} + (\mathbf{e}_m^q \cdot \ddot{\mathbf{x}}^q - \mathbf{e}_m^r \cdot \ddot{\mathbf{x}}^r) + \left(\frac{1}{\rho_m^q}\left[\left|\dot{\mathbf{x}}_m^q\right|^2 - (\dot{\rho}_m^q)^2\right] - \frac{1}{\rho_m^r}\left[\left|\dot{\mathbf{x}}_m^r\right|^2 - (\dot{\rho}_m^r)^2\right]\right) &= \mathbf{e}_m^{q,r} \cdot \ddot{\mathbf{x}}_m \\
-\ddot{\rho}_m^{r,s} + (\mathbf{e}_m^r \cdot \ddot{\mathbf{x}}^r - \mathbf{e}_m^s \cdot \ddot{\mathbf{x}}^s) + \left(\frac{1}{\rho_m^r}\left[\left|\dot{\mathbf{x}}_m^r\right|^2 - (\dot{\rho}_m^r)^2\right] - \frac{1}{\rho_m^s}\left[\left|\dot{\mathbf{x}}_m^s\right|^2 - (\dot{\rho}_m^s)^2\right]\right) &= \mathbf{e}_m^{r,s} \cdot \ddot{\mathbf{x}}_m
\end{aligned}
\tag{2.2.16}
$$

This system of equations can be written as:

$$
\mathbf{a} = \mathbf{E}_a \ddot{\mathbf{x}}_m \tag{2.2.17}
$$

where $\mathbf{E}_a$ is a matrix with three rows and three columns comprised of the transposed, between satellite differenced direction vectors in (2.2.16), and **a** is a vector with three rows comprised of the left hand side of (2.2.16).

Equation (2.2.17) can be solved as:

$$
\ddot{\mathbf{x}}_m = \mathbf{E}_a^{-1}\mathbf{a} \tag{2.2.18}
$$

Again, note that the $\ddot{\rho}_m^{p,q}$ terms were computed by double differencing $\ddot{\phi}_m^p$, $\ddot{\phi}_m^q$, $\ddot{\phi}_k^p$, and $\ddot{\phi}_k^q$ and adding single difference on receiver 'k' calculated with Equation (2.2.9), remembering that the acceleration of the base receiver 'k' is zero. With Equation (2.2.18) the unique solution for the receiver antenna acceleration is acquired.

Taking a qualitative look at the system of equations in (2.2.16), it can be seen that the errors in relative velocity are attenuated by the division by the receiver-satellite range. Thus, errors in the relative velocity solutions can be well tolerated. Also note that since $\dot{\phi}_m^p$ will be corrupted by satellite and receiver clock terms, the $\dot{\rho}_m^p$ term in the centrifugal terms is computed using the relative velocity solution and Equation (2.2.7). Since the magnitude of the satellite accelerations is quite small, errors in their measure are of concern. Errors could be proportionally large and will be propagated with no reduction through the inner product with the direction vector. Errors in $\ddot{\rho}_m^p$ ($\ddot{\phi}_m^p$) are also of concern, but are mitigated by the double differencing process.

In summary, the carrier method as presented in Jekeli and Garcia (1997) uses only four satellites in the acceleration solution. While the equations shown imply that only between-satellite differencing is done, double differencing is in fact applied, with the single difference being manufactured from calculations. The double differencing is necessary to eliminate the clock terms and to reduce errors from atmospheric delays. Differentiation of the carrier phases eliminates the carrier phase ambiguity, as it is constant. Cycle slips must be corrected, or else the derivative will be corrupted by edge effects around the discontinuity in the carrier phases, caused by the cycle slip. The quality of receiver positions used is not critical, with 10 m accuracy being tolerable. However, the quality of satellite velocities and accelerations are important and should be derived carefully from the precise ephemeredes for the highest possible accuracy.

Chapter 3

Modification of the Carrier Method

The carrier method, as presented in Section 2.2, provides an alternative to the position method of estimating accelerations. However, it can be improved upon, to increase its robustness. Limiting it to a unique solution does not allow for error minimization, meaning all errors remaining in the carrier phase derivatives and satellite information will map directly into the acceleration estimates. According to estimation theory, more measurements should lead to better estimates, particularly if the measurements are weighted properly. Therefore, the carrier method is modified to utilize a least squares solution, such that all available measurements are used. In addition, since the quality of the carrier phase measurements from different satellites varies, a covariance model was also developed and incorporated in the least squares solution.

This modified carrier method should provide some advantages over the position method. Namely, it will allow for a minimization of errors in the acceleration domain. Tracing the effect of measurements from one satellite into the acceleration solution is simplified, as the algorithm directly combines carrier phase measurements to estimate acceleration. As with the original carrier method, positioning requirements are relaxed, matching the level required for normal gravity computations. Also, using a least squares solution potentially allows for quality measures to be provided with the acceleration estimates.

In this chapter, the modification of the carrier method will be presented. In Section 3.1, Equations (2.2.15) and (2.2.18) are extended to provide a least squares solution for the relative remote station-satellite velocity and remote station acceleration. To provide appropriate weighting of the measurements, a covariance model is developed and is presented in Section 3.3. The model is applicable to both carrier phases and their derivatives. A technique for propagating carrier phase variances through the differentiation process is presented. Since this technique requires an understanding of the differentiation process, Section 3.2 first addresses issues surrounding differentiation of

the carrier phases and details the differentiating filter used herein. Section 3.4 provides justification that the modified carrier method is indeed an improvement over the original.

3.1 Least Squares Realization of the Carrier Method

To use all available measurements, from 'n' satellites, Equations (2.2.15) and (2.2.18) can be modified to create a least squares solution. Using the least squares technique (Mikhail, 1976), the relative velocity and acceleration solutions can be realized with a parametric model. Since both solutions are linear with respect to the parameters, no iteration is required. The relative velocity solution becomes:

$$\dot{\mathbf{x}}_m^p = (\mathbf{E}^T \mathbf{C}_{DD\dot{\phi}}^{-1} \mathbf{E})^{-1} \mathbf{E}^T \mathbf{C}_{DD\dot{\phi}}^{-1} \mathbf{b} \tag{3.1.1}$$

where $\mathbf{C}_{DD\dot{\phi}}$ is the covariance matrix of the double differenced first carrier phase derivatives, and all other quantities are as defined in Equation (2.2.15).

The remote station acceleration becomes:

$$\ddot{\mathbf{x}}_m = (\mathbf{E}_a^T \mathbf{C}_{DD\ddot{\phi}}^{-1} \mathbf{E}_a)^{-1} \mathbf{E}_a^T \mathbf{C}_{DD\ddot{\phi}}^{-1} \mathbf{a} \tag{3.1.2}$$

where $\mathbf{C}_{DD\ddot{\phi}}$ is the covariance matrix of the double differenced second carrier phase derivatives, and all other terms are as defined in Equation (2.2.18).

3.2 Differentiator Selection

The first step in processing is obtaining the carrier phase derivatives. The carrier phase derivatives are the measurements in the carrier method, and their quality determines the quality of the acceleration estimate. The choice of differentiator is a very important consideration. FIR filters are considered exclusively, as a constant phase delay over all frequencies is required to time tag the data properly. Additionally, only odd length

differentiating filters are used to maintain an integer time delay (Oppenheim and Schafer, 1999). A non-integer time delay would require interpolation.

When applying a differentiator, consideration must be given to the spectral properties of both the signal and the differentiator. While the ideal differentiator amplifies with increasing frequency, realizable FIR differentiators of odd length can only approximate the ideal case within a certain bandwidth, above which it attenuates the signal. This practical constraint of differentiator design is useful, as it can be used to suppress noise, particularly in low dynamic applications. Figure 3.2.1 illustrates the frequency responses of various orders of Taylor approximation differentiators, which are also referred to as central difference equations, at a 1 Hz sampling rate. (The filter order herein is the number of samples on either side of the central sample used in the differentiator, and is consistent with GPS literature. In signal processing literature, the filter order is defined as the filter length minus one.)

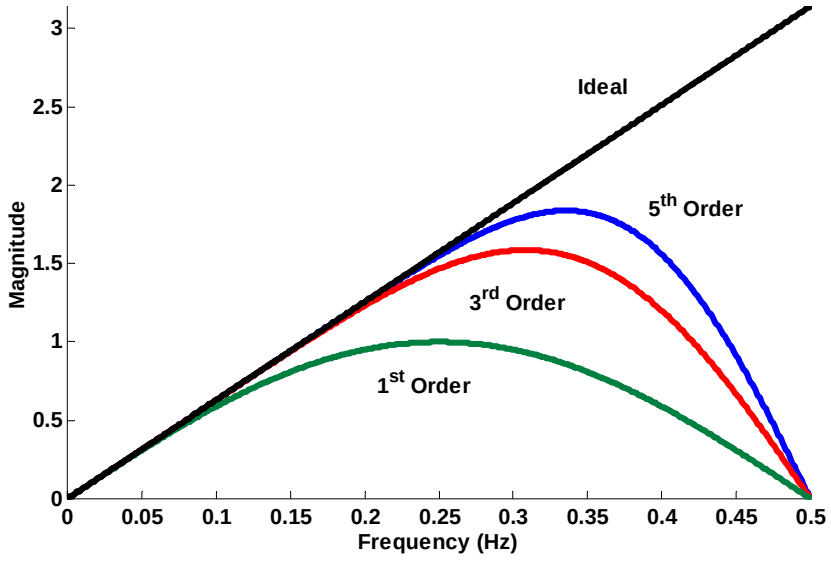

Figure 3.2.1 Magnitude of the frequency responses of various orders of Taylor approximation differentiators, and the ideal differentiator, with 1 Hz sampling rate

As can be seen in Figure 3.2.1, a differentiating filter can also act as a low pass filter for frequencies above its effective bandwidth. The bandwidth of the differentiator must

approximate the ideal case in the bandwidth corresponding to the motion of the aircraft, but can be designed to suppress noise if its bandwidth is no wider than necessary. The danger in using a differentiator with a very narrow bandwidth, or smoothing before differentiation, is that higher frequency motion of the aircraft may not be captured, resulting in a poor estimate of the derivative. Using a wider bandwidth ensures that all aircraft motion will be retained, but more noise will also be allowed to pass into the derivative. Figure 3.2.2 illustrates this in the frequency domain.

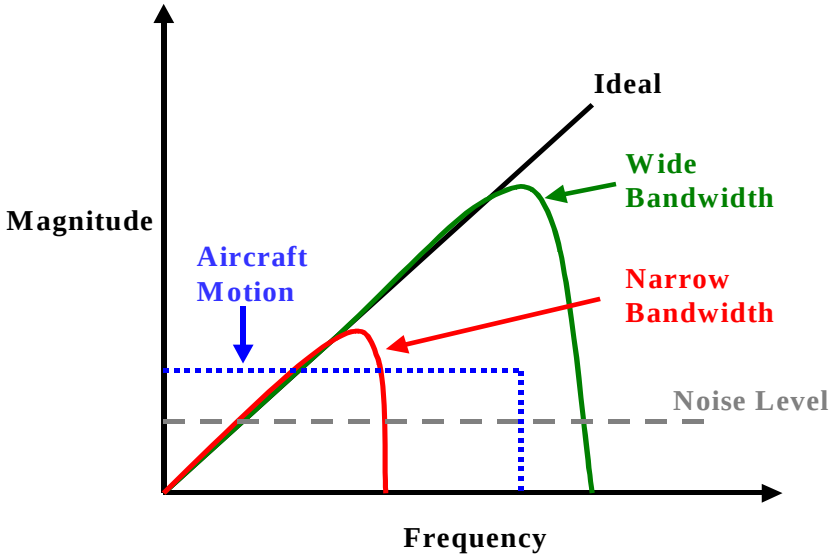

Figure 3.2.2 Frequency domain representation of the effect of narrow and wide differentiator bandwidths

As a compromise between sufficient bandwidth, simplicity, and noise suppression, a 5th order Taylor approximation differentiator was chosen. To compute the carrier phase derivatives, the carrier phases were convolved with the impulse response of the 5th order Taylor approximation. Beyer (1980) provides closed form formulas for the computation of higher order Taylor approximation impulse responses. The impulse response for the 5th order Taylor approximation is:

$$\mathbf{h}_5[n] = \frac{1}{T}\left[\frac{1}{1260} \quad \frac{-5}{504} \quad \frac{5}{84} \quad \frac{-5}{21} \quad \frac{5}{6} \quad 0 \quad \frac{-5}{6} \quad \frac{5}{21} \quad \frac{-5}{84} \quad \frac{5}{504} \quad \frac{-1}{1260}\right] \quad (3.2.1)$$

where T is the sampling rate of the data to be differentiated.

Uniform sample spacing is required for the application of the differentiator. Careful receiver selection, or extra data processing, is required to meet this requirement. Nominally, the carrier phases are logged with uniform time spacing (i.e. 1 Hz data). However, this assumption may not hold when the receiver clock resets to GPS time. The reset to GPS time changes the receiver clock offset by up to one millisecond, most commonly, but the reset can be larger. If the reset is large (i.e. 1 millisecond), the integration period over which the carrier phase measurement is formed is shorter or longer than the nominal output rate by the amount of the receiver clock reset. This results in the carrier phase measurement being either too large or too small by the amount of the receiver clock reset multiplied by the Doppler. If the Doppler on a satellite is high, a "mini" cycle slip is created. For example, if the receiver is measuring a Doppler of 3000 Hz on a satellite, and the clock reset is 1 ms, the carrier phase measurement will be off by 3 cycles. These "mini" cycle slips can be corrected as the size and time of the clock reset is known. If they are not corrected, edge effects will occur in the carrier phase derivatives.

GPS receivers generally fall into two groups with respect to how the clock resets are implemented. One group allows the receiver clock offset to drift as much as 1 millisecond and then resets in one epoch. If this type of receiver is used, the extra data processing described above is required. The other group uses clock steering and adjusts the clock offset at each epoch, by much smaller increments, on the order of hundreds of nanoseconds. With receiver clock resets of this size, the sample spacing can be considered uniform as the effect on the measured carrier phases is very small. Figure 3.2.3 shows the receiver clock offsets of an Ashtech Z-12 receiver, while Figure 3.2.4 shows the receiver clock offsets of a NovAtel MiLLennium receiver, which implements epoch-to-epoch clock steering as a user selected option. Note the different scale in each plot on the vertical axis, which shows the clock offset in terms of meters, calculated as the speed of light multiplied by the clock offset in seconds.

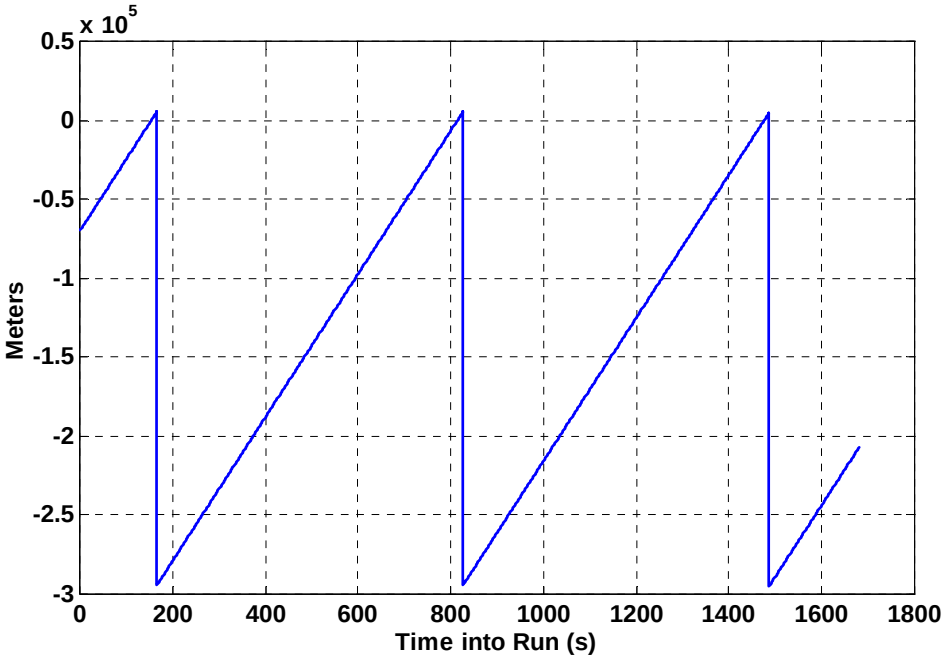

Figure 3.2.3 Ashtech Z-12 receiver clock offsets

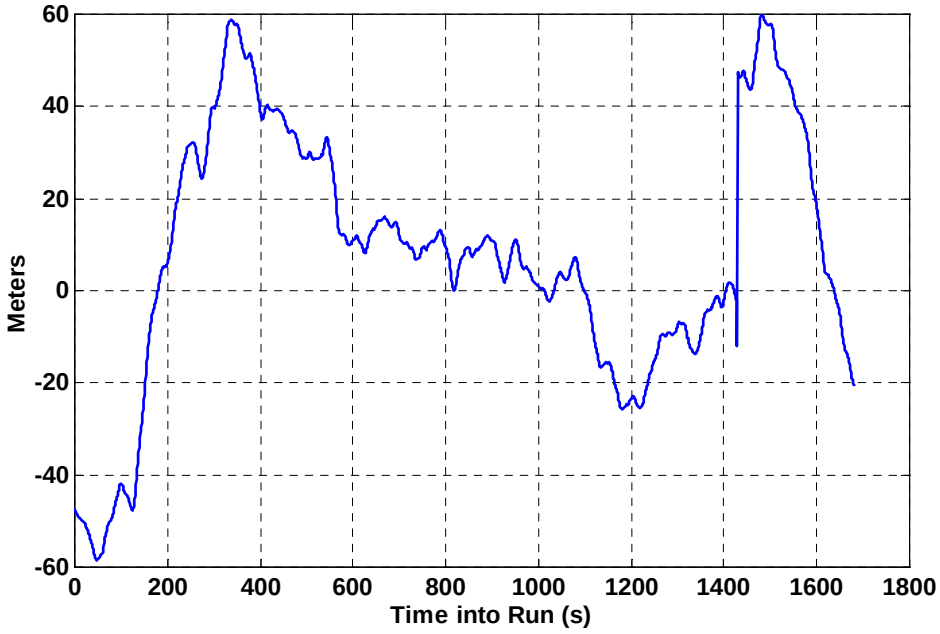

Figure 3.2.4 NovAtel MiLLennium receiver clock offsets

3.3 Covariance Model

GPS signals from different satellites do not have uniform quality. With an appropriate covariance model, poor quality signals can still be used, with much lower weighting than higher quality signals. Atmospheric effects on GPS measurements are a major error source. Measurements from low elevations satellites suffer the most degradation due to the atmosphere, as their path length through the atmosphere is longest. Elevation based weighting is commonly employed to assign increasing variance with decreasing elevation. What is not often incorporated is the covariance between measurements. Signals traveling similar paths through the atmosphere will have correlated atmospheric errors and this characteristic is exploited in double differencing, which also removes the clock errors. The covariance model developed for the modified carrier method uses elevation based weighting and models the covariance between measurements due to tropospheric and ionospheric variances. Physical and mathematical correlations are taken into account.

Further refinements in the covariance model are definitely possible. However, the focus of this thesis is the comparison of the carrier and position methods of acceleration determination. An adequate, but not necessarily ideal, covariance model is required for testing the carrier method. The covariance model developed herein provided reasonable results and was deemed adequate for the purposes at hand.

The tropospheric modeling is patterned after the method presented in Radovanovic et al. (2001). A similar scheme is added for ionospheric error variances, using the ionospheric mapping function outlined in Skone (1998). The variance of a single measurement, from one satellite to one receiver is modeled as:

$$\sigma_k^{p\,2} = m_T(\varepsilon_p)^2\sigma_T^2 + m_I(\varepsilon_p)^2\sigma_I^2 + \sigma_{multi}^2 \tag{3.3.1}$$

where σ_T^2, σ_I^2 are the tropospheric and ionospheric variances, respectively,

σ_{multi}^2 is the multipath variance,

ε_p is the elevation angle to satellite 'p',

m_T is the tropospheric mapping function, from the UNB3 model (Collins, 1999), and

m_I is the ionospheric mapping function (Skone, 1998) and given as:

$$m_I(\varepsilon) = [1 - [\cos\varepsilon(1 + \frac{h}{R_e})^{-1}]^2]^{-\frac{1}{2}} \qquad (3.3.1a)$$

where h is the height of the ionospheric shell (350 km) and R_e is the Earth's radius.

Figure 3.3.1 shows the mapping function values with respect to elevation angle for both the ionospheric and tropospheric mapping functions.

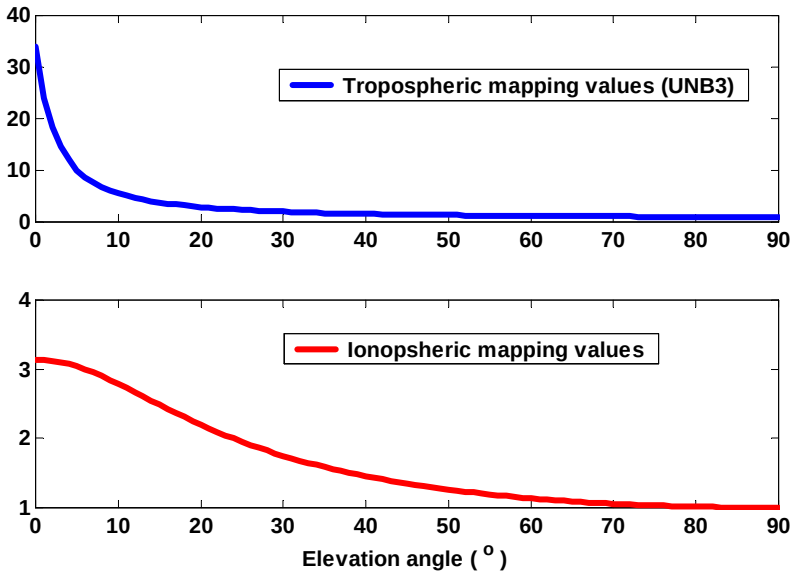

Figure 3.3.1 Tropospheric and ionospheric smapping functions

The covariance between measurements to two satellites from one receiver is modeled as:

$$\sigma_m^{pq} = m_T(\varepsilon_p) m_T(\varepsilon_q) \exp(-\theta/\Omega)\sigma_T^2 + m_I(\varepsilon_p) m_I(\varepsilon_q) \exp(-\theta/\Omega)\sigma_I^2 \qquad (3.3.2)$$

where θ is the separation angle between satellites 'p' and 'q', and is calculated as:

$$\cos\theta = \sin\varepsilon_p \sin\varepsilon_q + \cos\varepsilon_p \cos\varepsilon_q \cos(A_p - A_q) \qquad (3.3.2a)$$

A_p, A_q are the azimuths to satellites ‘p’ and ‘q’ and

Ω is the correlation angle.

The correlation angle controls the amount of covariance modeled. As the angular separation of two satellites approaches, and exceeds, the value of the correlation angle, the magnitude of the calculated covariance decreases. The correlation angle value is chosen based on empirical testing of the specific dataset, as in Radovanovic et al. (2001).

A multipath term is not included in the covariance terms. Multipath is considered uncorrelated between different measurements in this covariance model. The base station antenna utilized a choke ring to minimize multipath. The multipath environment of the airborne receiver is difficult to quantify, since it is kinematic. Bruton (2000) estimates the effect of multipath in a typical airborne gravimetry environment to be approximately 0.3 cm, which is much smaller than the tropospheric and ionospheric effects, which may reach 10-15 cm and 1-2 m, respectively. The focus of this thesis was to compare the methods of acceleration determination rather than to develop a rigorous covariance model. Thus, the modeling of correlated multipath error is left to future work.

Figure 3.3.2 shows the calculated covariance from Equation (3.3.2) between satellite pairs at low, mid, and high elevation angles, where $\sigma_T^2 = 0.02^2\ \mathrm{m}^2$, $\sigma_I^2 = 0.05^2\ \mathrm{m}^2$ and $\Omega = 40^o$.

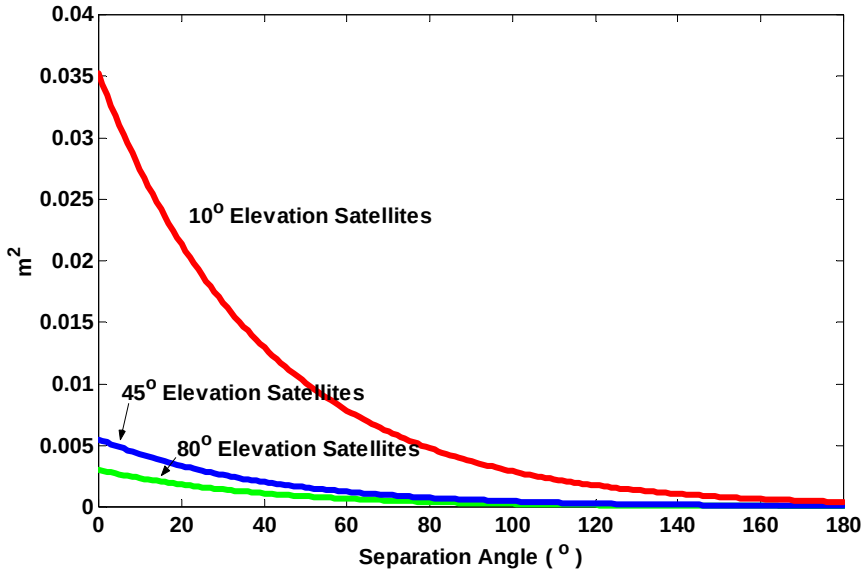

Figure 3.3.2 Covariance values for measurements from one receiver to two satellites

The covariance between measurements on two receivers from one satellite is modeled as:

$$\sigma_{mk}^{p} = m_T(\varepsilon_p)^2 \exp(-d/D)\sigma_T^2 + m_I(\varepsilon_p)^2 \exp(-d/D)\sigma_I^2 \qquad (3.3.3)$$

where d is the separation distance between receivers and

D is the correlation distance.

Similarly to the correlation angle, the correlation distance limits the covariance between measurements to one satellite from two receivers. The correlation distance is often taken to be 350 km (Radovanovic et al., 2001), but other values could be used, based on either empirical testing of the data or atmosphere models. If the receiver separation is more than the correlation distance, the covariance computed from Equation (3.3.3) will not be significant.

Figure 3.3.3 shows the covariance computed, using Equation (3.3.3), the same ionospheric and atmospheric variances as in Figure 3.3.2, and D = 350 km.

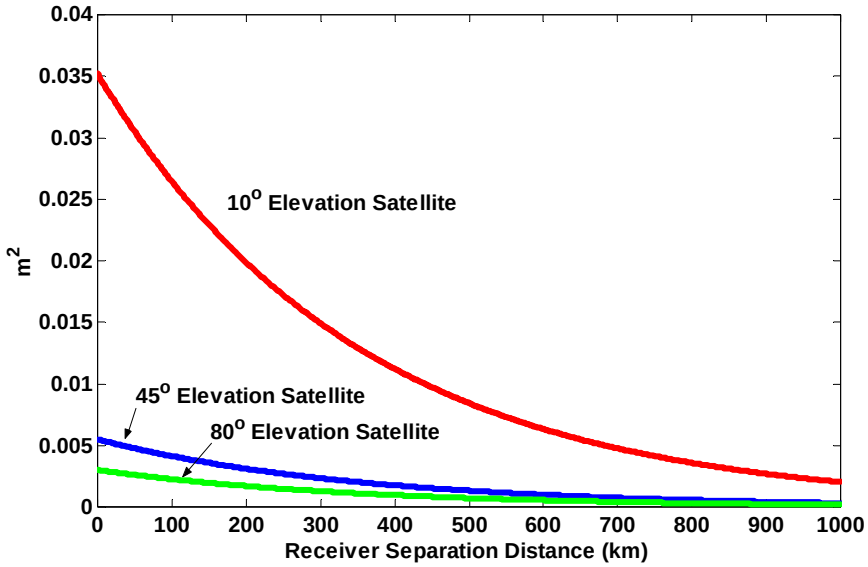

Figure 3.3.3 Covariance values computed for measurements from one satellite to two receivers, separated by the values on the horizontal axis

The covariance between two measurements, each to a different satellite from a different receiver is:

$$\sigma_{mk}^{pq} = m_T(\varepsilon_p) m_T(\varepsilon_q) \exp(-\theta/\Omega) \exp(-d/D) \sigma_T^2 + m_I(\varepsilon_p) m_I(\varepsilon_q) \exp(-\theta/\Omega) \exp(-d/D) \sigma_I^2 \qquad (3.3.4)$$

Figure 3.3.4 shows the covariance values from Equation (3.3.4) for two measurements from different receivers to different satellites, with the same ionospheric and tropospheric variances as before and receiver separation of 100 km, which is a typical baseline length in airborne gravimetry.

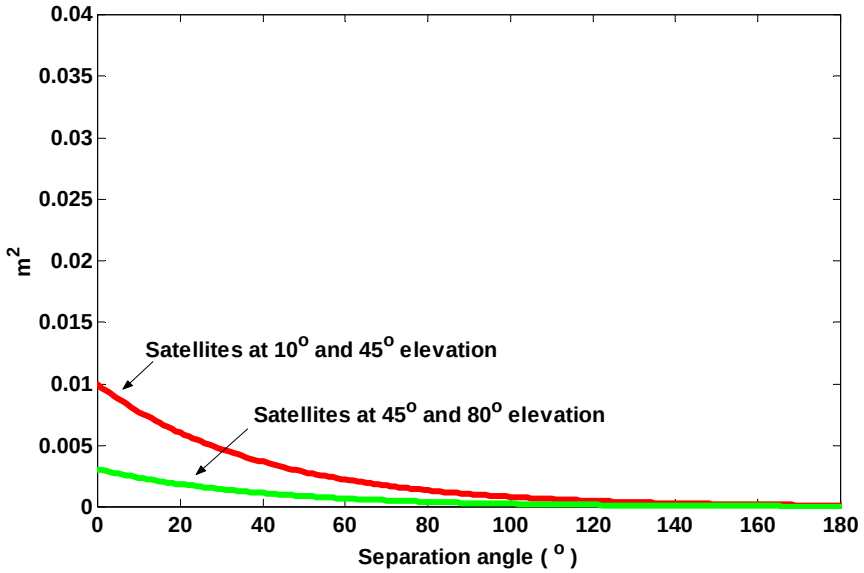

Figure 3.3.4 Covariance values computed for two measurements from different satellites to different receivers, separated by 100 km

A fully populated, symmetric covariance matrix results from using Equations (3.3.1) through (3.3.4). For example, the case of measurements from three satellites on two receivers would have a covariance matrix of the form:

$$\mathbf{C}_{\phi} = \begin{bmatrix} \sigma^{2\,p}_{m} & \sigma^{pq}_{m} & \sigma^{pr}_{m} & \sigma^{p}_{mk} & \sigma^{pq}_{mk} & \sigma^{pr}_{mk} \\ \sigma^{qp}_{m} & \sigma^{2\,q}_{m} & \sigma^{qr}_{m} & \sigma^{qp}_{mk} & \sigma^{q}_{mk} & \sigma^{qr}_{mk} \\ \sigma^{rp}_{m} & \sigma^{rq}_{m} & \sigma^{2\,r}_{m} & \sigma^{rp}_{mk} & \sigma^{rq}_{mk} & \sigma^{r}_{mk} \\ \sigma^{p}_{km} & \sigma^{pq}_{km} & \sigma^{pr}_{km} & \sigma^{2\,p}_{k} & \sigma^{pq}_{k} & \sigma^{pr}_{k} \\ \sigma^{qp}_{km} & \sigma^{q}_{km} & \sigma^{qr}_{km} & \sigma^{qp}_{k} & \sigma^{2\,q}_{k} & \sigma^{qr}_{k} \\ \sigma^{rp}_{km} & \sigma^{rq}_{km} & \sigma^{r}_{km} & \sigma^{rp}_{k} & \sigma^{rq}_{k} & \sigma^{2\,r}_{k} \end{bmatrix} \tag{3.3.5}$$

When the measurements are differenced, the mathematical correlations must be accounted for. A new covariance matrix is formed by propagating the variances of the individual measurements into the differenced measurements.

$$\mathbf{C}_{\phi DD} = \mathbf{B}_{DD}\mathbf{C}_{\phi}\mathbf{B}^{T}_{DD} \tag{3.3.6}$$

where each row of the $\mathbf{B}_{DD}$ matrix contains the coefficients of the differencing equation used to form the double differences.

However, it is carrier phase derivatives that are double differenced in the carrier method. The carrier phase derivatives calculated with an FIR filter are just linear combinations of the carrier phases. Therefore, the variance of the carrier phase derivatives can be related to the variance of the carrier phases using the same variance propagation technique used for differenced carrier phases. The equation for propagating the carrier phase variances into the derivatives is:

$$\mathbf{C}_{\dot{\phi}} = \mathbf{B}_{filter}\mathbf{C}_{\phi-filter-length}\mathbf{B}_{filter}^{\mathbf{T}} \tag{3.3.7}$$

The rows of $\mathbf{B}_{filter}$ contain the impulse response of the chosen differentiator, padded with zeros such that it only operates on the time series of one measurement. $\mathbf{C}_{\phi-filter-length}$ is a block diagonal matrix, with the blocks made up of the covariance matrices for a measurement set for one epoch. The variances and covariances for a measurement set for one epoch are based on elevation. If changes in elevation can be considered insignificant over half the length of the filter, the computations can be simplified. With typical kinematic data rates being a minimum of 1 Hz, this is a valid assumption. Each block in $\mathbf{C}_{\phi-filter-length}$ will be identical, as the changes in the elevation-based variances can be considered negligible. It can be shown that:

$$\mathbf{C}_{\dot{\phi}} = \sum_{0}^{n}\mathbf{h}[n]^2\mathbf{C}_{\phi} \tag{3.3.8}$$

$$\mathbf{C}_{\ddot{\phi}} = \sum_{0}^{n}\mathbf{h}[n]^2\mathbf{C}_{\dot{\phi}} = (\sum_{0}^{n}\mathbf{h}[n]^2)^2\mathbf{C}_{\phi} \tag{3.3.9}$$

To illustrate this, consider the case of measurements from two satellites to two receivers, with the 1st order Taylor approximation used as the differentiator. The first-order Taylor approximation impulse response with unit sample spacing (1 Hz) is:

$$\mathbf{h}_1[n] = \begin{bmatrix} -0.5 & 0 & 0.5 \end{bmatrix} \tag{3.3.10}$$

$\mathbf{B}_{filter}$, using the 1st order Taylor approximation impulse response, is:

$$\mathbf{B}_{filter(4,12)} = \begin{bmatrix} -0.5 & 0 & 0 & 0 & 0 & 0 & 0 & 0 & 0.5 & 0 & 0 & 0 \\ 0 & -0.5 & 0 & 0 & 0 & 0 & 0 & 0 & 0 & 0.5 & 0 & 0 \\ 0 & 0 & -0.5 & 0 & 0 & 0 & 0 & 0 & 0 & 0 & 0.5 & 0 \\ 0 & 0 & 0 & -0.5 & 0 & 0 & 0 & 0 & 0 & 0 & 0 & 0.5 \end{bmatrix} \tag{3.3.11}$$

In this case $\mathbf{C}_{\phi-filter-length}$ is:

$$\mathbf{C}_{\phi-filter-length(12x12)} =$$

$$\begin{bmatrix} \sigma^{2\,p}_{m} & \sigma^{pq}_{m} & \sigma^{p}_{mk} & \sigma^{pq}_{mk} & & & & & & & & \\ \sigma^{qp}_{m} & \sigma^{2\,q}_{m} & \sigma^{qp}_{mk} & \sigma^{q}_{mk} & & & 0 & & & & 0 & \\ \sigma^{p}_{km} & \sigma^{pq}_{km} & \sigma^{2\,p}_{k} & \sigma^{pq}_{k} & & & & & & & & \\ \sigma^{qp}_{km} & \sigma^{q}_{km} & \sigma^{qp}_{k} & \sigma^{2\,q}_{k} & & & & & & & & \\ & & & & \sigma^{2\,p}_{m} & \sigma^{pq}_{m} & \sigma^{p}_{mk} & \sigma^{pq}_{mk} & & & & \\ & 0 & & & \sigma^{qp}_{m} & \sigma^{2\,q}_{m} & \sigma^{qp}_{mk} & \sigma^{q}_{mk} & & & 0 & \\ & & & & \sigma^{p}_{km} & \sigma^{pq}_{km} & \sigma^{2\,p}_{k} & \sigma^{pq}_{k} & & & & \\ & & & & \sigma^{qp}_{km} & \sigma^{q}_{km} & \sigma^{qp}_{k} & \sigma^{2\,q}_{k} & & & & \\ & & & & & & & & \sigma^{2\,p}_{m} & \sigma^{pq}_{m} & \sigma^{p}_{mk} & \sigma^{pq}_{mk} \\ & 0 & & & & 0 & & & \sigma^{qp}_{m} & \sigma^{2\,q}_{m} & \sigma^{qp}_{mk} & \sigma^{q}_{mk} \\ & & & & & & & & \sigma^{p}_{km} & \sigma^{pq}_{km} & \sigma^{2\,p}_{k} & \sigma^{pq}_{k} \\ & & & & & & & & \sigma^{qp}_{km} & \sigma^{q}_{km} & \sigma^{qp}_{k} & \sigma^{2\,q}_{k} \end{bmatrix} \tag{3.3.12}$$

Multiplying $\mathbf{B}_{filter}\mathbf{C}_{\phi}\mathbf{B}^{T}_{filter}$ gives:

$$\mathbf{C}_{\dot{\phi}} = \mathbf{B}_{filter}\mathbf{C}_{\phi}\mathbf{B}_{filter}^{T} = (0.5^2 + 0.5^2)\begin{bmatrix} \sigma^{2\,p}_{m} & \sigma^{pq}_{m} & \sigma^{p}_{mk} & \sigma^{pq}_{mk} \\ \sigma^{qp}_{m} & \sigma^{2\,q}_{m} & \sigma^{qp}_{mk} & \sigma^{q}_{mk} \\ \sigma^{p}_{km} & \sigma^{pq}_{km} & \sigma^{2\,p}_{k} & \sigma^{pq}_{k} \\ \sigma^{qp}_{km} & \sigma^{q}_{km} & \sigma^{qp}_{k} & \sigma^{2\,q}_{k} \end{bmatrix} \tag{3.3.13}$$

For the second derivative, the same process is repeated, as the filter is applied in cascade. This technique of propagating variances is valid for any FIR filter. The pre-multiplier for $\mathbf{C}_{\dot{\phi}}$ and $\mathbf{C}_{\ddot{\phi}}$ will change for each differentiating filter applied.

It is interesting to note that the scale factor increases as the bandwidth of the differentiator increases. The scale factor for the fifth-order Taylor approximation is 1.51, which is larger than the first-order scale factor of 0.50, and the third-order scale factor of 1.17. At first it seems counterintuitive that the first-order Taylor approximation of the differentiator reduces variance. However, a look at the frequency response of the first-order Taylor differentiator, in Figure 3.2.1, confirms it is similar to a low pass filter – at no point does the gain exceed unity. Also, the scale factor derived from the variance propagation corresponds to the magnitude of the frequency response when the differentiator begins to diverge from the ideal.

Any covariance model developed for carrier phases can be used for the carrier phase derivatives by applying the derivative variance propagation explained above. If improved covariance models are available, they can be easily implemented in the carrier method of acceleration determination.

Lastly, $\mathbf{C}_{\dot{\phi}DD}$ and $\mathbf{C}_{\ddot{\phi}DD}$ can be formed in the same way $\mathbf{C}_{\phi DD}$ was formed in Equation (3.3.6), having found expressions for $\mathbf{C}_{\dot{\phi}}$ and $\mathbf{C}_{\ddot{\phi}}$.

If only the parameter estimates are of interest $\mathbf{C}_{\phi}$ can be used as $\mathbf{C}_{\dot{\phi}}$ and $\mathbf{C}_{\ddot{\phi}}$ to increase computational efficiency. The scale factor due to the differentiation could be applied similarly to an a priori variance factor. Changing the a priori variance factor will not

change the parameter estimates. It will affect the accompanying statistical quantities, like the estimated parameter variances and the residuals, which could be computed with the a priori variance factor, if these quantities were of interest.

Least square statistical quantities, such as the estimated acceleration variance and the residuals, have not been used to evaluate the acceleration estimates in this thesis, as comparison to the independent reference gravity field was used for the accuracy evaluation. The calculated parameter variances potentially could be used for quality control, indicating periods when the acceleration estimates are poor, thus allowing the user to view the gravity disturbance estimates critically. In the covariance modeling presented, the tropospheric and ionospheric zenith variance remain constant. The parameter variances would reflect the geometry of the solution. There is no mechanism to check if the signal quality has degraded beyond what was modeled. Carrier to Noise (C/No) measurement made by the receiver have been used in covariance modeling (Hartinger and Brunner, 1999). C/No is a receiver dependent quantity and is a relative measure only. A possible use in this instance would be to increase the variance of measurements further if the C/No measure changed suddenly, which could indicate a change in signal quality.

3.4 Implementation Details

To clarify how the carrier method can be implemented in practice, the details of the processing will be presented in this section.

The algorithm and covariance model described in Sections 3.1 to 3.3 is realized in a software package called CABA (**CA**rrier **B**ased **A**ccelerations) developed entirely by the author in C++, with some utilities in Matlab™. It is a self contained program requiring the precise ephemeris file in SP3 format, a text file of remote receiver positions, and raw GPS files for the master and remote stations in GPB format, which is used by the KINGSPAD software package developed at the University of Calgary.

Figure 3.4.1 shows the processing flow of the modified carrier method as implemented in CABA, with a detailed description of each processing step in the following text.

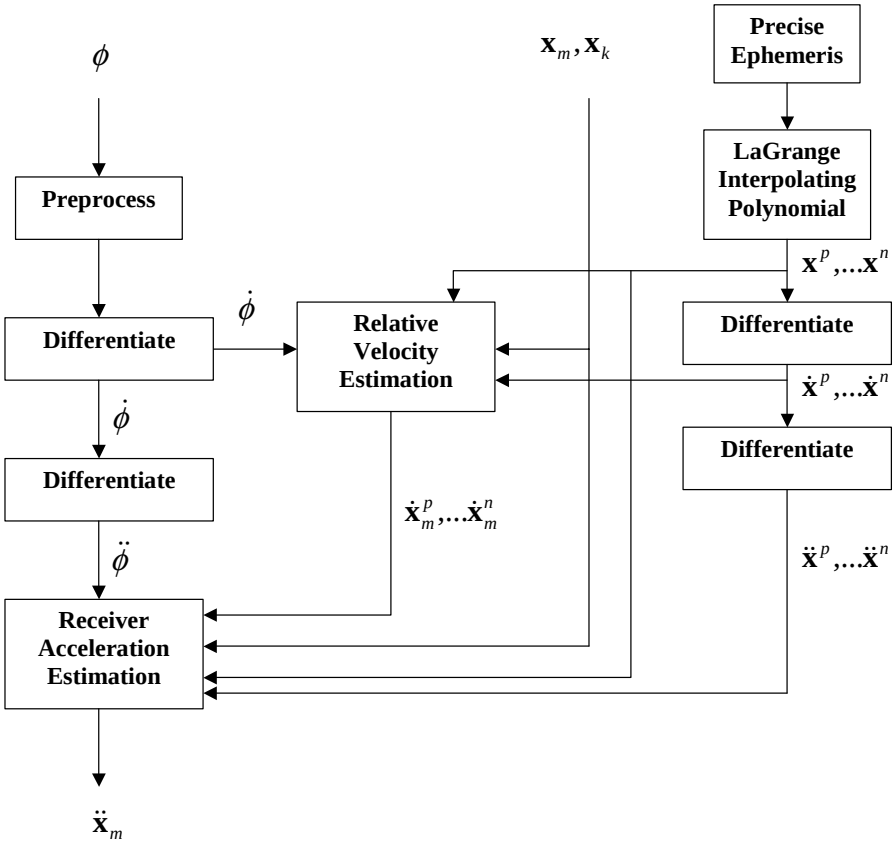

Figure 3.4.1 Flowchart of modified carrier method of acceleration estimation

There are two main modules within CABA. The first module performs the preprocessing and differentiation. Before the modified carrier method algorithm can be implemented, the carrier phases require preprocessing, which includes checking for cycle slips and receiver clock resets, along computing a value for the ionospheric variance. Cycle slips must be detected and corrected. The velocity trend, or range rate, method was used (Hoffmann-Wellenhof, 2001).

However, correcting cycle slips is not a trivial matter. The carrier method proved to be an excellent test as to whether a cycle slip was properly identified and corrected. If a cycle slip is incorrectly fixed, the resulting receiver acceleration estimate clearly shows this, with a large spike at the time of the improper fix. While processing, slips of several cycles were found and "fixed", but spikes in the acceleration estimates showed that the apparent slips were in fact due to motion, as leaving them unmodified removed the acceleration spike problem. Figure 3.4.2 shows an example of the acceleration spikes caused by an incorrect cycle slip detection and fix.

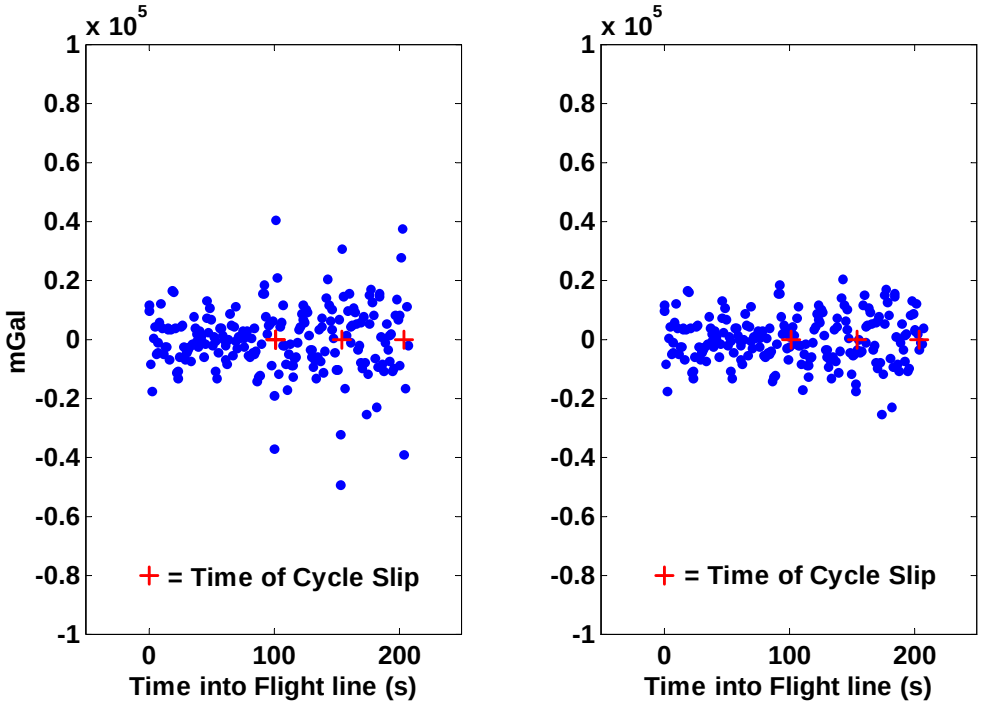

Figure 3.4.2 Acceleration spikes caused by incorrect cycle slip fixing: the left hand plot shows the receiver accelerations when apparent cycle slips were fixed, while the right hand plot shows the accelerations computed without any cycle slip fixing

The threshold used for cycle slip detection has to be selected specifically for flight conditions, being much higher during turbulent flights than during smooth flights. Cycle slips due to signal blockage are not a concern, as knowledge of the ambiguities is not needed in the carrier method.

To avoid dealing with cycle slips and eliminate one level of differentiation, one might consider using the raw Doppler as the first carrier phase derivative. The raw Doppler can be much noisier than a derived Doppler (Cannon et al., 1997, Szarmes et al., 1997). However, the first carrier phase derivatives are only used to compute the relative velocity solution, which does not have to be extremely accurate. Recalling the discussion in Section 2.2, the magnitude of relative velocity squared is divided by the receiver satellite separation distance in the acceleration Equation (2.2.16). For mGal accuracy accelerations, the error in the relative velocity magnitude could be up to 10 m/s. The problem lies in obtaining the second carrier phase derivatives by differentiating the noisier raw Doppler measurements. Low pass filtering could be applied; although, this would have to be investigated to insure it would leave the aircraft motion signal intact while still removing the noise. The dynamics of airborne gravimetry are generally quite low, making cycle slips a rare occurrence. In this testing, cycle slips were not a problem and the most accurate carrier phase derivatives were desired, such that the best possible acceleration estimates could be obtained. Hence, carrier phase derivatives were computed from the carrier phase measurements rather than the Doppler measurements.

Receiver clock resets are also of concern, as explained in Section 3.1. For this reason, NovAtel MiLLennium receivers were used in this research, because they implement clock steering. If receivers without clock steering are used, the receiver clock reset times and the magnitude of the resets need to be known. Using the Doppler measurement on each satellite and the size of the clock reset, the phase data could be corrected in a similar fashion to a cycle slip. CABA currently does not include this option, but it could be added without much difficulty.

The final step in preprocessing is estimating the ionospheric variance, for use in the covariance model. The ionosphere changes frequently so this variance is computed for each flight line. Dual frequency data was collected, allowing for the computation of the first order ionospheric error. To quantify the ionospheric error variation from epoch to epoch (1 Hz data rate) the L1 and IF phase measurements were converted to meters. The two were then differenced to give the first order ionospheric error. A line of best fit was

removed from this difference to leave only the variations from first order. This quantity gives the second and higher order effects of the ionosphere and the carrier phase noise, increased by the differencing and formation of the IF measurement. The variance of it is used as the ionospheric variance, which will be pessimistic given the increased noise level and inclusion of multipath. The highest elevation satellite for each flight line is selected and its computed ionospheric variation is mapped to the zenith, using the mapping function given in Section 3.2.

The tropospheric variance was not changed for each flight line. It remained constant, at 0.02^2 m^2. The multipath variance was also held constant at 0.005^2 m^2. The correlation angle was 40 degrees for all flight lines, while the correlation distance was 350 km. These values were chosen based on Radovanovic et al. (2001). They could likely be refined to improve the covariance model, but provided reasonable results for the objectives of this research.

After the preprocessing is complete, differentiation can be performed. The carrier phase data is convolved with the impulse response of the differentiator. In this case, a fifth-order Taylor approximation was used, as discussed in Section 3.1. Care must be taken to properly time tag the derivatives. The time of the derivative is the time of the carrier phase measurement that the central sample of the differentiator lies upon. For example, when using the fifth-order Taylor differentiator, the first valid derivative would be time tagged to match the sixth carrier phase measurement. This differentiation, and corresponding time tagging, is performed via convolution with the impulse response of the chosen differentiator as the final step in the first module of CABA.

The other differentiation that occurs in the modified carrier method is that of the satellite positions. Precise ephemeris provides the satellite positions and clock offsets every 15 minutes. The satellite positions are required at each computation epoch, which in this work was every second. Lagrange polynomials (9^{th} order) are used to interpolate the satellite positions, as in Hoffmann-Wellenhof (2001). The satellite velocities and accelerations are also required at each computation epoch. Numerical differentiation is

not very practical in this circumstance, as it would require several satellite positions to be interpolated. The Lagrange polynomials can be analytically differentiated. Their form is known and the chain rule can be applied (and programmed) to produce their derivative function, which then is evaluated at the computation epoch. This functionality is part of the second module of CABA, which performs the modified carrier method algorithm.

With all the data sources explained, the relative velocity and receiver acceleration computations can be performed as shown in Figure 3.4.1 and described in Equations (2.2.13), (2.2.16), (3.1.1) and (3.1.2). This final step is the main purpose of the second module of CABA.

3.5 Justification of the Modifications to the Carrier Method

Testing proved that the modifications to the carrier method were indeed improvements over the original carrier method. On every flight line tested the modified carrier method, with its least squares solution and covariance model, performed better than the unique solution of the original carrier method. Chapters 4 and 5 present the test methodology and results. Appendix A contains the results of the modified carrier method, which can be contrasted with the results from using a unique solution only, found in Appendix B. The unique solution performance is also discussed in Section 5.3. As well, when using all available satellites, the covariance model employed always improved the solution.

Chapter 4

Test Description

To compare the modified carrier and position method, testing under operational conditions was conducted. To be certain that differences were due purely to the method itself, both methods were tested using the same data. Since the goal was improved performance at the operational level, data from an airborne gravimetry campaign was used.

4.1 Test Area

The campaign was flown during the spring of 2000, over the Alexandria area between Montreal and Ottawa, Canada. The topography of the approximately 70 km by 120 km test area is minimal. Hence the gravity variations are due to density changes, making the field typical of areas where resource exploration would be pursued. There are significant variations in the gravity field, with disturbances ranging from -41 to 19 mGal at flying height. These values are given by the reference field, which was provided by Sander Geophysics Ltd. Figure 4.1.1 shows the reference gravity field for the test area, in contours.

The reference field was computed from upward continued ground measurements, which had an average spacing of three kilometers. The ground measurements were gridded on the ellipsoid and upward continued using a Fourier Transform technique. The accuracy of the reference field is expected to be at the mGal level. For more details about the reference field and the upward continuation method used, see Bruton (2000).

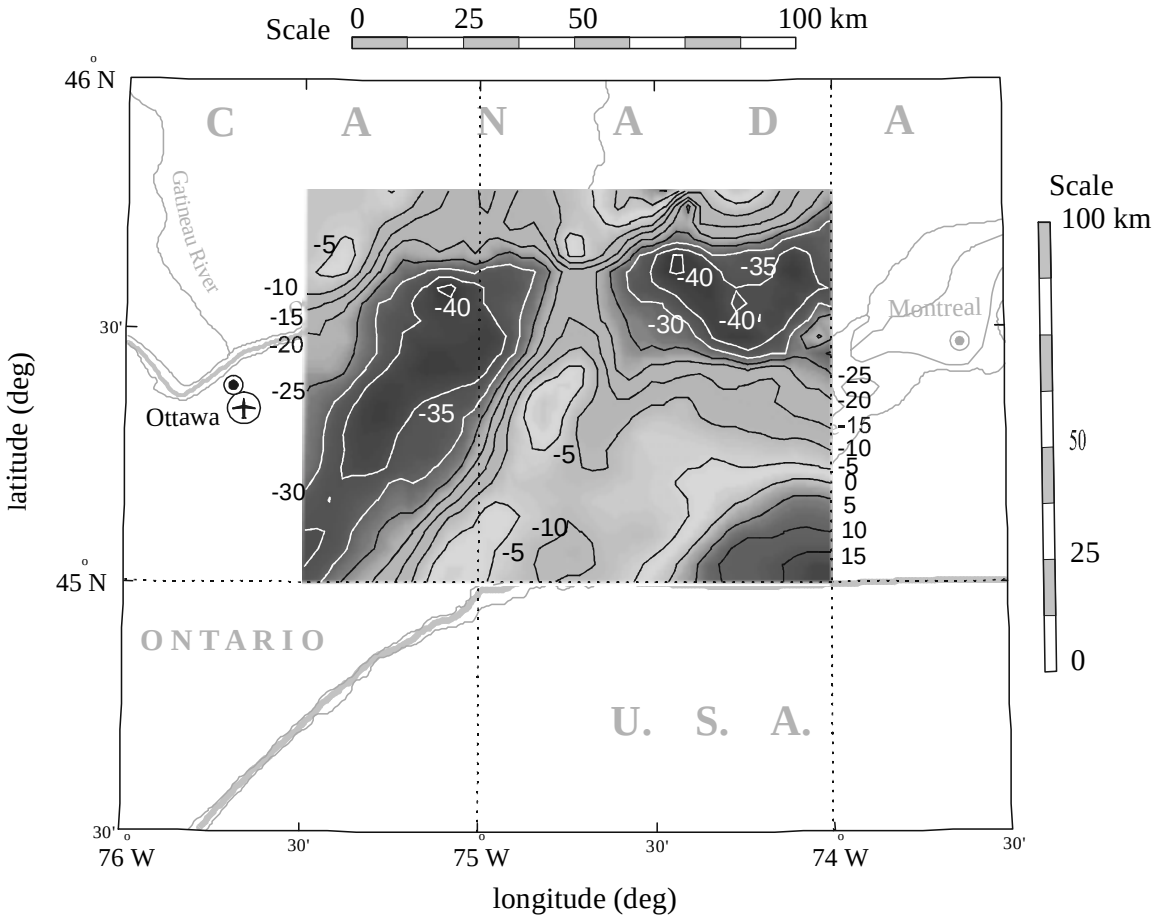

Figure 4.1.1 Reference gravity field for the Alexandria test area

4.2 Flight Conditions

During this campaign, the flight height was approximately 500 meters above the ground with a flying speed of 45 m/s, on average. Each flight line was about 90 km in length. Herein, four flight lines were selected for testing. They were chosen because they were repeated on two days of flying that had contrasting GPS measurement conditions, giving a total of eight lines for analysis. Increased levels of ionospheric activity degrade GPS signals. The ionosphere follows a diurnal pattern of activity, with the peak occurring around 14:00, local time.

On the first day, April 19, the flights took place from 11:00 and 15:00, local time, when the ionosphere was very active. The second day's flights, on May 4, were flown in the

early morning, from 04:30 to 07:30, when the ionosphere activity was quite low. The different flight times allow for comparison under different ionospheric activity levels, as the ionosphere is most active in the early afternoon and quite calm during the early morning. Levels of ionospheric activity were verified in two ways. Firstly, dual frequency data was collected and the ionospheric free observable was formed and compared to the L1 measurements. Secondly, geomagnetic data from the Ottawa observatory, located immediately east of the city, was checked and it confirmed the conclusions drawn from the GPS data.

In addition, the April 19 flights experienced moderate to high flight turbulence, while the May 4 flights had extremely smooth flying conditions. The overall conditions of April 19 would generally be considered too extreme for a high quality, operational airborne gravimetry flight. However, this data provides an opportunity to examine the effect of the ionosphere and flight turbulence on the estimated gravity disturbances. Figure 4.2.1 shows the flight lines used in this analysis. The GPS base station is located at the Ottawa airport. Baseline lengths did not exceed 70 km.

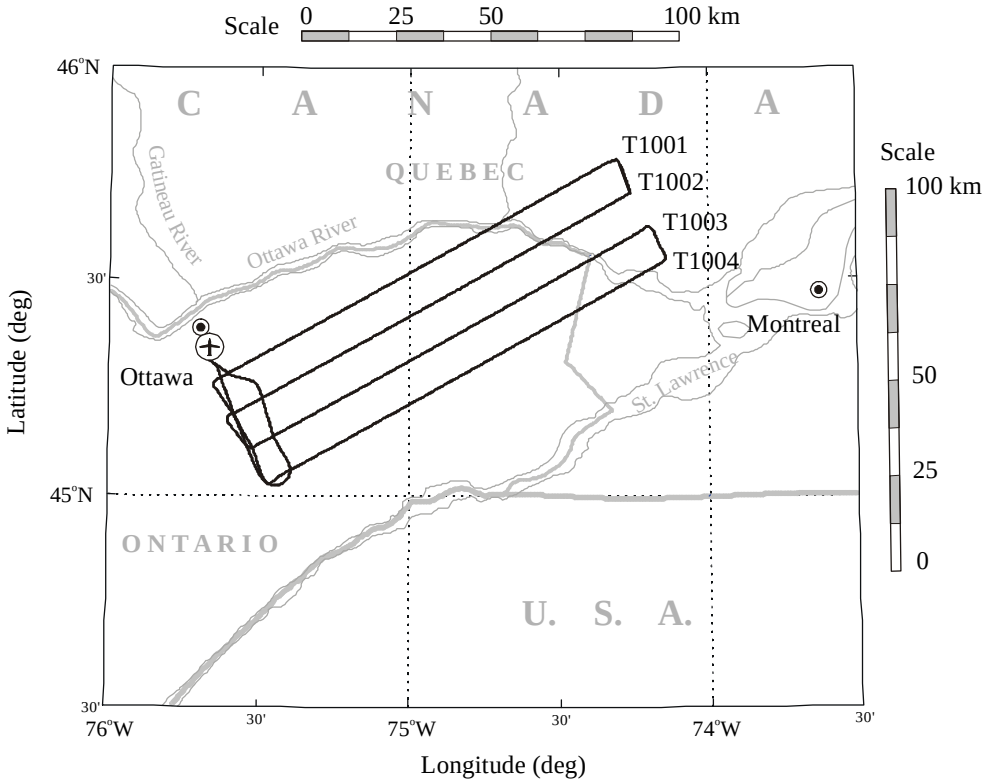

Figure 4.2.1 Flight lines

4.3 Equipment

An off-the-shelf SINS, a Honeywell LRF III, was used as the gravimeter. For the technical specifications of the LRF III, see (Glennie, 1999). Dual frequency NovAtel MiLLenium receivers collected 10 Hz data on the aircraft and at the base station, which was provided by Sander Geophysics Ltd. This data was downsampled to 1 Hz for processing. The aircraft was a Cessna Caravan. GPS data was also collected with Ashtech Z-12 receivers. The two receivers shared the same antenna.

4.4 Processing

The aircraft positions were processed by A. Bruton and results are discussed in Bruton, (2000). The position estimates resulted from differential carrier phase processing, with ambiguities fixed in widelane mode, using the GrafNav™ software package. These

position solutions are the best possible, in the context of airborne gravimetry and the length of the baselines. The available satellite constellation was closely monitored and controlled, to prevent any discontinuities in the position trajectory. Forward and reverse time position solutions were processed and compared to show errors caused by the initialization or loss of satellites.

The raw GPS data for the position solution was collected with Ashtech Z-12 receivers. The carrier method processing used raw GPS data from NovAtel MiLLennium receivers. The receivers collecting data on the aircraft and the base station shared the same antenna, meaning they collected the same signals. The differences in noise level in the two receivers should not be significant in this testing, as they are of the same grade.

For each flight line, two sets of aircraft accelerations were estimated: one with the position method and one with the modified carrier method. The modified carrier method is realized in a software package developed by the author called CABA, which was described in Section 3.4. This package consists of two modules. The first performs the preprocessing, which includes cycle slip detection and fixing, and differentiation of the carrier phase measurements. The second module implements the modified carrier method, as described in Chapter 3 and shown in Figure 3.4.1.

With these two sets of accelerations, two sets of gravity disturbances were computed, using the AGFILT module of the GREATGUN software package developed at the University of Calgary. This process is shown below in Figure 4.4.1.

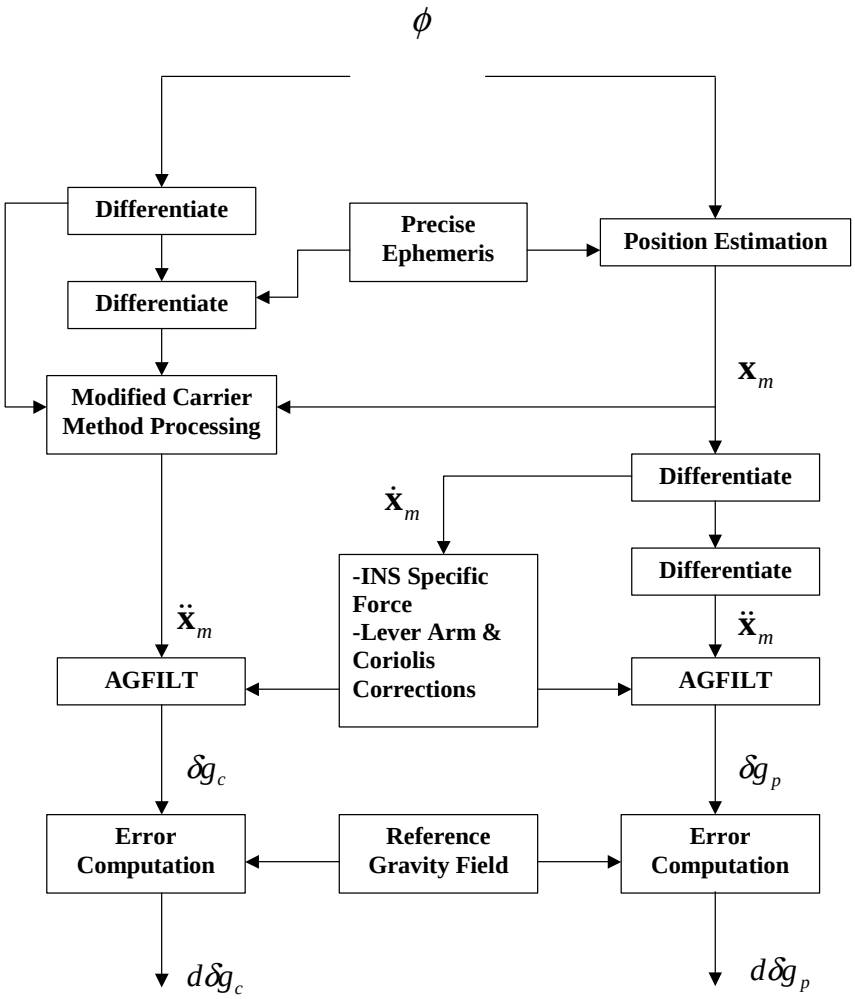

Figure 4.4.1 Flowchart of the processing to compare the modified carrier and position methods of acceleration estimation

Several sets of gravity disturbances were generated as the output of the above process, with filtering periods of 30, 60, 90 and 120 seconds. The spatial resolutions corresponding to these filtering periods, and the campaign flight speed of 45 m/s, are given in Table 4.4.1.

Table 4.4.1 Spatial Resolutions corresponding to filtering period

1/*fc* (s)	**30**	**60**	**90**	**120**
Spatial Resolution (km)	0.7	1.4	2.0	2.7

4.5 Evaluation Criteria

The error in the estimated gravity field is dominated by the errors in the GPS accelerations; therefore, comparison to the reference gravity field gives an indication of the accuracy of the GPS accelerations. The gravity disturbances computed with both methods of acceleration determination were evaluated with respect to agreement to the reference field, which shows accuracy differences. The reference field also contains error and this will be included in the error attributed to the gravity disturbance estimates. Moreover, a portion of the error attributed to the estimates at high frequency is due to their higher frequency content, which the reference does not contain. Hence, the errors given for the gravity disturbance estimates are somewhat pessimistic.

Since the emphasis of this research is on high frequency performance, a linear trend, with respect to the reference, was removed from the gravity disturbance estimates. The reported error is given by the standard deviation of differences between the estimated gravity disturbances and the reference. Better agreement is indicated by a lower standard deviation.

Before continuing on to the numerical results, it is useful to compare both methods of acceleration estimation at the conceptual level. Figure 4.5.1 shows a schematic of the position method, while Figure 4.5.2 shows the schematic of the carrier method.

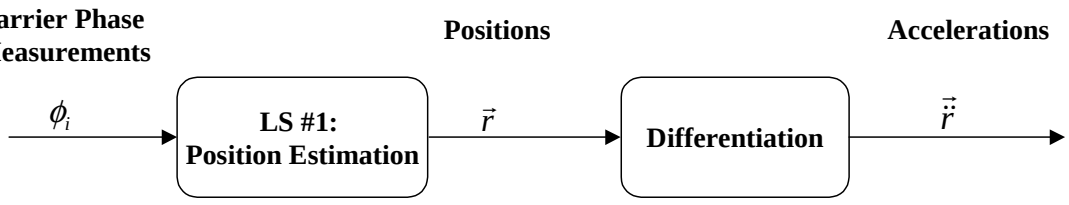

Figure 4.5.1 Schematic of Position Method of Acceleration Estimation

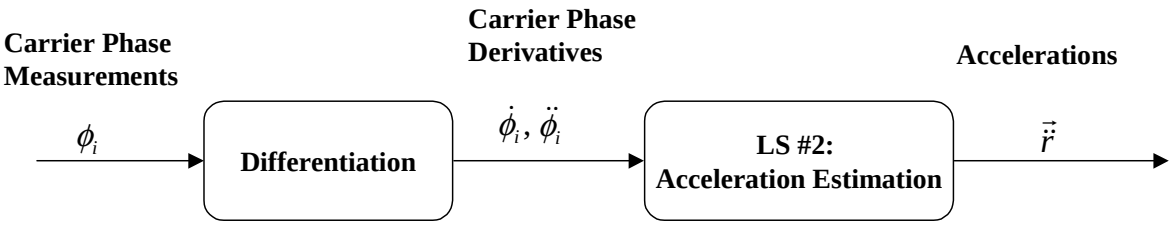

Figure 4.5.2 Schematic of Carrier Method of Acceleration Estimation

Comparison of Figures 4.5.1 and 4.5.2 shows that there is no conceptual difference in the two methods of acceleration estimation. Viewing the two methods from a signal processing perspective, if least squares estimation and differentiation can both be considered linear time invariant filters, there should be no difference in the final output, whatever the order of application. Therefore, the differences between the results of the position and carrier methods are not expected to be large. However, a numerical comparison is necessary to examine any differences under operational conditions.

Chapter 5

Results and Analysis

In this section, results showing the modified carrier phase method's performance under various conditions are presented. The performance of the modified carrier phase method is tested under conditions of changing satellite constellations, low quality positions, low satellite availability, and varying levels of ionospheric activity. Additionally, the effect of differentiator bandwidth is discussed in Section 5.5. For clarity, representative results are selected and presented in the text, while the complete set of results are provided in the Appendices. Evaluation of the results is based on comparison with the position method and the reference gravity field, as described in Chapter 4.

5.1 Effect of Changing Satellite Constellation

In previous work (Bell et al., 1999, Bruton, 2000, Brozena and Childers, 2000), it has been shown that the gain or loss of a satellite can degrade the position solution. In turn, this affects the acceleration solution derived by differentiating the series of estimated positions. Often the effect of this change in geometry is a jump in the position trajectory. Although this does not pose a problem in the position domain, even small discontinuities cause large edge effects once differentiated into the acceleration domain.

To avoid this problem when using the position method, the user must carefully process the GPS positions to hold the constellation constant throughout a flight line. Not only does this increase the amount of user input required for processing, it also disregards available satellites that should be able to contribute to the solution. Since the rise or fall of a satellite is a common occurrence, and affects the quality of the acceleration solution derived from differentiating positions, the effect on the modified carrier phase method is of interest. If the modified carrier method can smoothly accommodate changing geometry, while matching or improving agreement to the reference field, it has a significant operational advantage over the position method.

Tables 5.1.1, 5.1.2, and 5.1.3 show the error of the scalar gravity disturbances computed with modified carrier phase method, with respect to the reference gravity field, on flight lines T1002 and T1003 flown on April 19, 2000 and flight line T1003 flown on May 4, 2000. All three flight lines had changes in the visible satellite constellation in the modified carrier method processing. The position method results were processed to avoid constellation changes during the flight line.

Table 5.1.1 Errors (1 σ) of estimated δg_u with respect to the reference field (mGal) for T1002 flown on April 19, 2000

Method	30s	60s	90s	120s
Carrier	9.28	2.63	1.63	1.38
Position	11.26	2.73	1.88	1.54

Table 5.1.2 Errors (1 σ) of estimated δg_u with respect to the reference field (mGal) for T1003 flown on April 19, 2000

Method	30s	60s	90s	120s
Carrier	27.74	4.83	1.97	1.52
Position	27.76	4.81	2.00	1.52

Table 5.1.3 Errors (1 σ) of estimated δg_u with respect to the reference field (mGal) for T1003 flown on May 4, 2000

Method	30s	60s	90s	120s
Carrier	6.28	2.38	2.02	1.89
Position	8.85	3.07	2.23	1.95

Figures 5.1.1, 5.1.2 and 5.1.3 correspond to Tables 5.1.1, 5.1.2 and 5.1.3, graphically showing the results for the 90s filtering period.

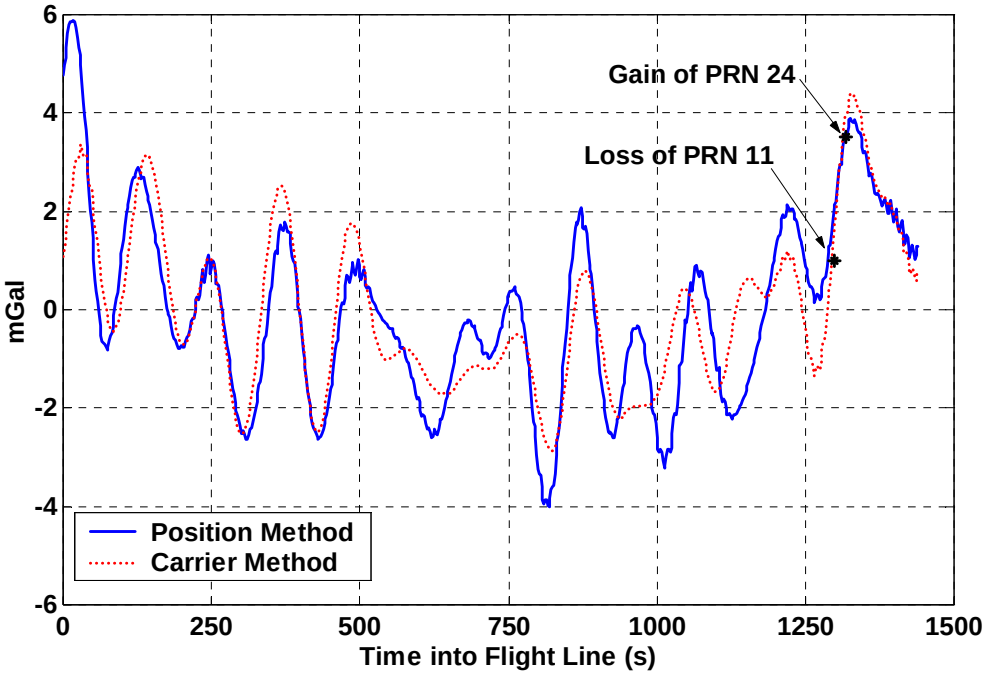

Figure 5.1.1 Error of estimated δg_u, with respect to the reference field, for T1002 on April 19, 2000 with a 90s filter applied

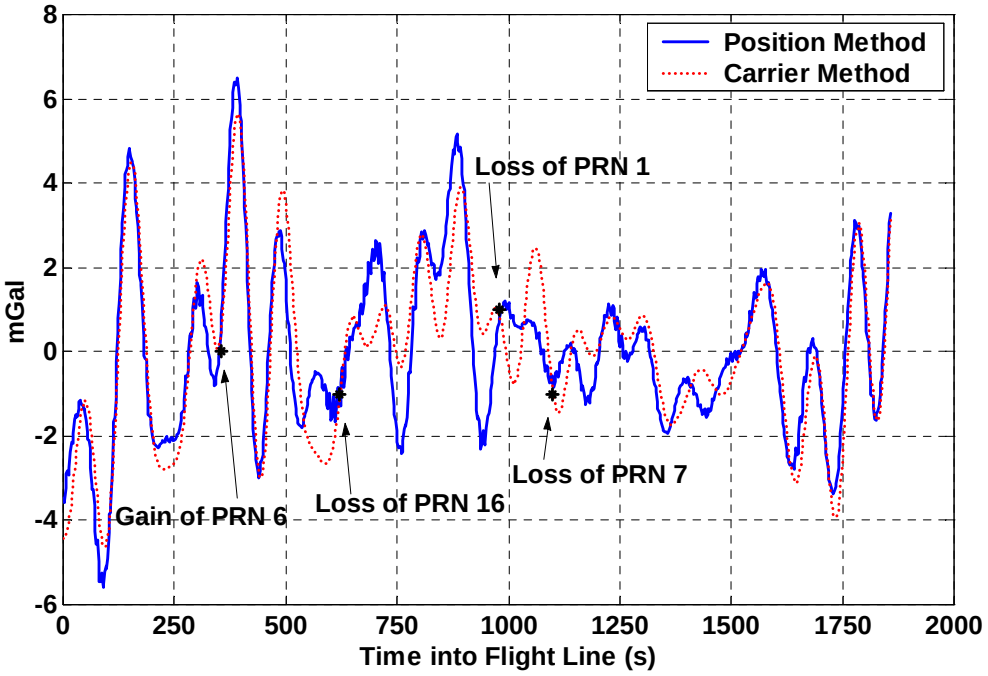

Figure 5.1.2 Error of estimated δg_u, with respect to the reference field, for T1003 on April 19, 2000 with a 90s filter applied

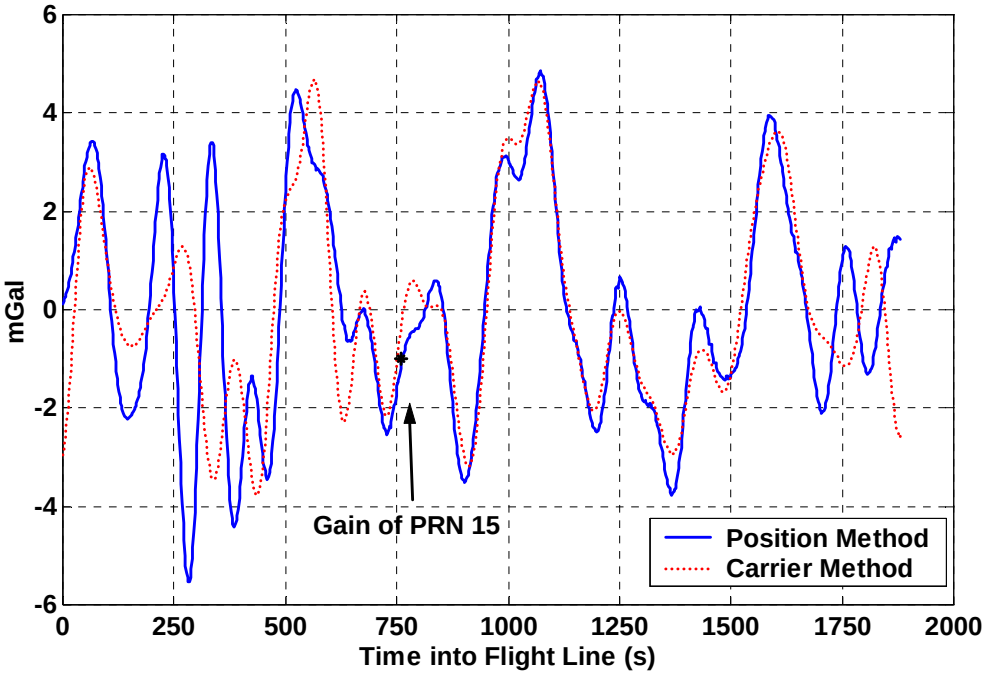

Figure 5.1.3 Error of estimated δg_u, with respect to the reference field, for T1003 on May 4, 2000 with a 90s filter applied

Changing the satellite constellation did not negatively impact the gravity disturbance solution, as can be seen by the carrier results shown above. The modified carrier method provides a better agreement to the reference field than the position method for two flight lines, at all filtering levels, and matches the results for the third. Introducing or losing a satellite does not upset the gravity disturbance solution. This was observed for all eight flight lines and the complete set of results, with flight information, is given in Appendix A. The improvement is typically small, which was foreseeable considering the conceptual similarity in the acceleration determination methods explained in Section 4.5.

To determine if the smooth introduction or elimination of a satellite is due to the covariance model, gravity disturbances were processed using accelerations computed with the modified carrier method without the covariance model.

If the covariance model is not incorporated in the carrier method, gains and losses are not handled well, particularly when fewer satellites are available. When many (nine or more) satellites are available, the disturbance caused by a geometry change is minimal. Flights

T1002 and T1003 of April 19 illustrate this well. Figure 5.1.4 shows the results of T1002 of April 19, processed without using the covariance model in the aircraft acceleration computations.

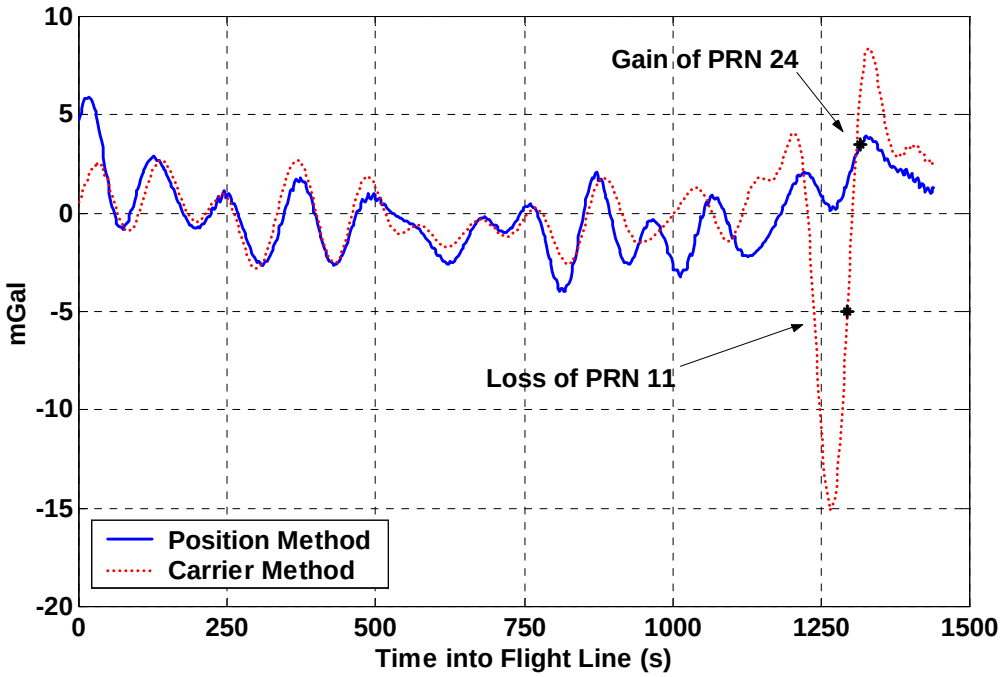

Figure 5.1.4 Error of estimated δg_u, with respect to the reference field, for T1002 on April 19, 2000 with a 90s filter applied and carrier method accelerations computed without a covariance model

During T1002 on April 19, the maximum number of satellites used in the acceleration solution was six. The loss of PRN 11 dropped the number to five for 20 seconds, until the gain of PRN 24. Processing T1002 without the covariance model, with the low number of available satellites and major geometry change, produced very poor results, with distinct upsets around the geometry changes. The errors are approximately eight times larger than when the covariance model was applied, as shown in Figure 5.1.1.

T1003 of April 19, processed without a covariance model used in the aircraft acceleration estimation, provides a good example of the lessened effect of geometry changes when there is high satellite availability. Figure 5.1.5 shows the results of processing the accelerations without the covariance model for T1003 of April 19.

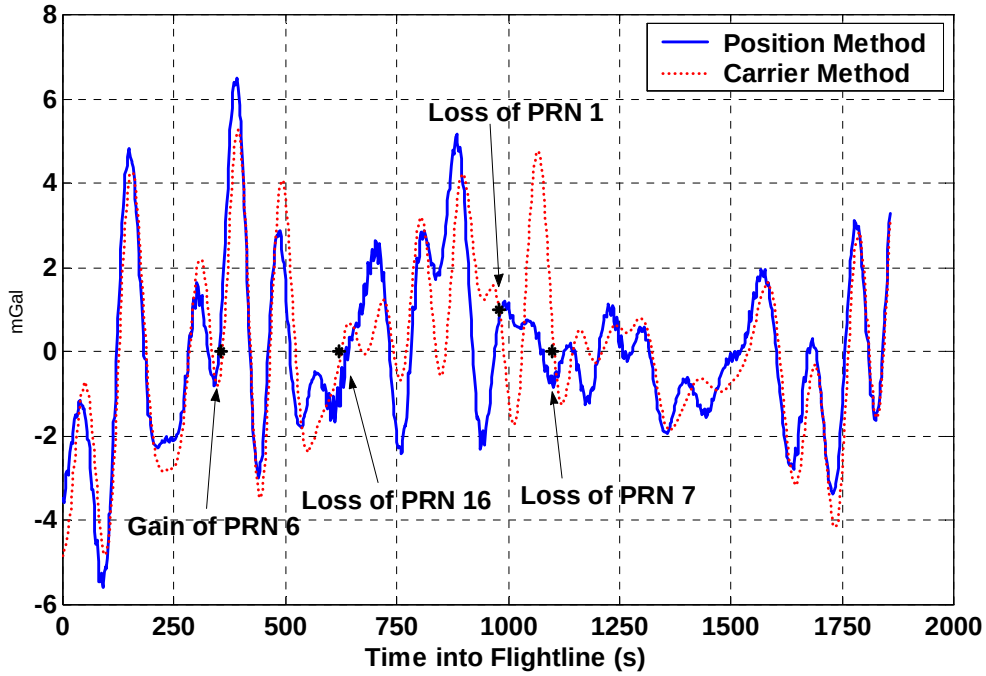

Figure 5.1.5 Error in estimated δg_u, with respect to the reference field, for T1003 on April 19, 2000 with a 90s filter applied and carrier method accelerations computed without a covariance model

The gain of PRN 6 brought the number of satellites used to 11, and had no significant impact on the error in the estimated gravity disturbances. The next three satellite losses show an increasing effect as the number of satellites used in the acceleration solution decreases. The first loss, of PRN 16, has little effect but the losses of PRN 1 and 7 cause greater errors as the number of satellites drops to eight. Comparing Figure 5.1.5 to 5.1.3 shows an approximately 2 mGal increase in error from the final two losses, without the application of the covariance model.

5.2 Use of Low Quality Positions

One of the potential strengths of the carrier phase method is its ability to tolerate lower quality positions. In the carrier phase method, the receiver antenna positions are used to calculate direction vectors to the satellites. Considering that the distance between them is over 20,000 km, even 10 m of positional error should be acceptable for sub-mGal accuracies (Jekeli, 1994). For one mGal acceleration accuracy, the position method requires positions accurate to the centimeter level (Wei et al., 1991). To achieve such

positioning accuracies with GPS, a differential, fixed ambiguity carrier phase solution is required.

Fixing ambiguities properly and reliably is not a trivial matter, entailing complex processing. For airborne gravimetry, abrupt changes in the position solution are not acceptable. The danger in fixing ambiguities is that a set may be chosen, used for sometime, and then residual tests will reveal that the chosen set is in fact incorrect. Then the ambiguity set must be re-estimated, resulting in a reversion to a float solution until fixing is again possible. This process can lead to jumps in position, or at the very least, a change in the estimated positions' standard deviation. Both effects will upset the acceleration solution derived from differentiating positions. Bruton (2000) recommended a float solution be used, except in circumstances of high resolution requirements and favorable GPS conditions.

In terms of processing, the differential code solution is easiest to obtain. There are no ambiguities to estimate. But the resulting position estimates are quite poor, with accuracies at best at the meter level, and realistically expected to be at the several meter level over longer baselines (i.e. 50 km and longer). This makes them unacceptable for use in the position method but not the carrier phase method, which has much lower positional accuracy requirements.

To test the response of each method to the use of lower quality positions, differential code positions were computed. On average the reported accuracy, by the processing software, of these code positions was 3-5 meters, with baselines not exceeding 65 km. Gravity disturbances were estimated using the code positions, in both the position method and the modified carrier phase method. In addition to comparing the methods, the results when using the best possible position solution (widelane fixed with no constellation changes), are also provided. Tables 5.2.1 and 5.2.2 show the results for each method, with both position solutions, on T1002 flown on April 19 and May 4, respectively.

Table 5.2.1 Errors (1 σ) of estimated δg_u with respect to the reference field (mGal) for T1002 flown on April 19, 2000, using high and low quality positions

Method	30s	60s	90s	120s
Carrier, with code positions	9.27	2.62	1.64	1.38
Carrier	9.28	2.63	1.64	1.38
Position, with code positions	394.40	116.83	42.20	21.19
Position	11.26	2.73	1.88	1.53

Table 5.2.2 Errors (1 σ) of estimated δg_u with respect to the reference field (mGal) for T1002 flown on May 4, 2000, using high and low quality positions

Method	30s	60s	90s	120s
Carrier, with code positions	8.34	1.69	1.24	1.16
Carrier	8.32	1.66	1.24	1.16
Position, with code positions	330.80	94.66	43.29	23.11
Position	7.43	2.47	1.30	1.17

These results clearly show that using code positions in the position method is unacceptable, as the errors increase by an order of magnitude. This was expected, as predicted by Equation (2.1.1), which relates positioning accuracy to acceleration accuracy. The position method using code positions was only processed on these two flight lines, since the results are not very meaningful beyond comparative purposes.

The carrier method performs equivalently with both position solutions. Appendix E contains the carrier method results with code position solutions for all flight lines, while Appendix A contains the results with the high quality position solutions for all flight lines. When using the carrier method the quality of the position solution is not critical, allowing the user to simplify his/her processing.

It must be noted that the carrier phase method does require carrier phase measurements of good quality. The carrier phase method provides the opportunity to use lower quality positions that result from less complex processing. However, if poor signal quality is the

cause of the low quality positions, the carrier phase method will not provide a good acceleration estimate.

5.3 Performance Under Low Satellite Availability

Under operational conditions, low satellite availability may be encountered. Even under these conditions, the quality of acceleration estimates should be maintained. The question is whether one method of acceleration determination is superior to the other during this situation.

To compare the position and carrier methods under low satellite availability, a unique set of four satellites was chosen for each flight line. The selection criteria for the satellite set was based on continual availability throughout the flight line, and best possible Dilution of Precision (DOP) values, which means as small as possible. Positions were processed using these four satellites to obtain a float solution, as it is not possible to fix ambiguities in this case. These positions were then used in both the position method and the carrier method to determine acceleration. The carrier method processing used the same four satellites used for the position solution.

From a total of eight flight lines, a direct comparison between the position and the carrier methods was only possible on seven of them. It was not possible to compute a unique position solution on T1001 of April 19, 2000 as GrafNav™ would not use one of the satellites due to poor signal quality for part of the line. Of the remaining seven flight lines, the carrier method performed better than the position method on six lines. The reason for the position method's comparatively better performance on the seventh line (T1004 of April 19) is unclear. On other flight lines with similar conditions, in terms of PDOP, VDOP and ionospheric activity, the carrier method fared better than the position method.

Table 5.3.1 shows the average performance, over all flight lines except T1001 of April 19, of both methods. Individual flight lines results are given in Appendix B.

Table 5.3.1 Average errors (1 σ) of estimated δg_u with respect to the reference field (mGal) over all lines, except T1001 of April 19, with a unique solution

Method	30s	60s	90s	120s
Carrier	24.24	6.11	2.86	2.03
Position	25.55	7.56	4.26	3.37

Although the carrier method generally performed better than the position method, it is not a reliable solution. In some instances, the acceleration estimate from the carrier method was grossly incorrect, and easily identifiable as such. One epoch's estimate could be up to two orders of magnitude in error. Inspection of the input data did not provide any indication of bad measurements or other disturbances that would cause such an erroneous estimate. It occurred on flight lines with varying conditions, making it impossible to isolate the conditions that caused the problem.

T1002 of April 19 provides a good example of this phenomenon, shown in the upward accelerations computed with different satellite sets in Figure 5.3.1. The top plot shows the accelerations computed with the unique satellite set of PRNs 2, 4, 9 and 16. The middle plot is a unique acceleration solution as well, with PRN 9 replaced by PRN 7. The bottom plot shows the accelerations computed with one degree of freedom, using PRNs 2, 4, 7, 9 and 16. Note the different scale used in the top plot on the vertical axis.

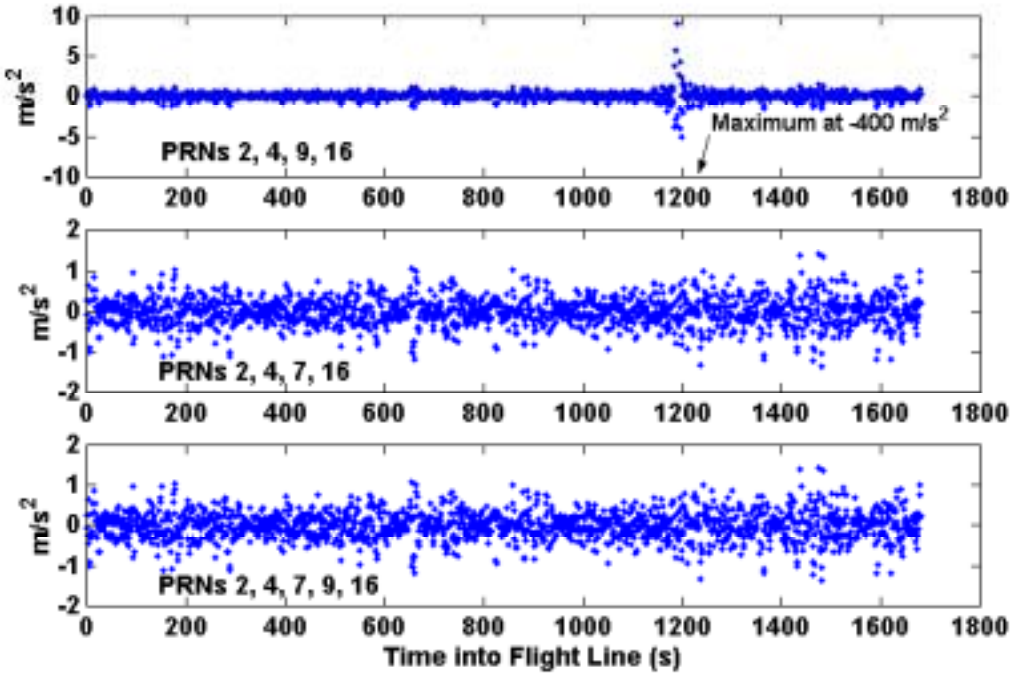

Figure 5.3.1 Upward aircraft accelerations computed with three satellite sets, as indicated on each plot, for T1002 of April 19, 2000

In the top plot of Figure 5.3.1, the erroneous acceleration estimates must be caused by PRN 9, as when it is replaced by PRN 7, in the middle plot, the problem disappears. This indicates a problem with the measurements on PRN 9, but none was apparent when examining these measurements.

In all cases, changing the satellite set allowed the flight line to be processed without the "spiking" problem. Also, as shown in the bottom plot of Figure 5.3.1, the addition of another satellite, to bring the total to just five, eliminated the problem as well. These last two observations suggest that the carrier method of estimating accelerations is very sensitive. When it is a unique solution, there is no way to minimize the errors and even a small error has a large impact on the estimated accelerations. The qualitative error analysis in Section 2.2 indicated that small errors in range accelerations computed from the carrier phases were of concern. The "spiking" problem in the case of a unique solution underlines the need for good signal quality in the carrier method.

5.4 Effect of Different Levels of Ionospheric Activity

The flights of April 19 and May 4 took place during mid-day and early morning, respectively. These two days of the campaign were chosen because of the flight times and the need to evaluate both methods under varying ionospheric conditions. Dual frequency data was collected, allowing for the computation of the first-order ionospheric error. To quantify the ionospheric error variation from epoch to epoch (1 Hz data rate) the L1 and IF phase measurements were converted to meters. The two were then differenced to give the first order ionospheric error. A line of best fit was removed from this difference to leave only the variations from first-order. This final quantity gives the second and higher order effects of the ionosphere and the carrier phase noise, increased by the differencing and formation of the IF measurement. The standard deviation of this quantity was computed for each satellite over each flight line. By taking the average of all satellites from a given flight line, an indication of the ionospheric activity was estimated.

The eight flight lines were grouped into two main categories of ionospheric activity, with one more extreme case. The T1001, T1002, and T1004 of May 4 formed the low ionospheric activity group, with an ionospheric standard deviation of 0.03 m, computed as described in the previous paragraph. T1003 of May 4, along with T1002, T1003 and T1004 of April 19, formed the moderate ionospheric activity group, with an ionospheric standard deviation of 0.05-0.06 m. T1001 of April 19 had a very high ionospheric standard deviation of 0.13 m. Table 5.4.1 summarizes the grouping according to ionospheric activity, as quantified by the ionospheric standard deviation. These categories correspond to the range of ionospheric activity encountered during this testing. What is considered “high” herein is not the highest possible level of ionospheric activity, but it is approaching the maximum level of tolerance for an airborne gravimetry flight.

Table 5.4.1 Flight lines grouped according to ionospheric activity level

High (0.13 m)	Moderate (0.05-0.06 m)	Low (0.03 m)
April 19: T1001	April 19: T1002	
	T1003	
	T1004	
	May 4: T1003	May 4: T1001
		T1002
		T1004

When the ionospheric variation was moderate to high, the carrier method consistently performed better than the position method at all filtering levels. Tables 5.1.1 and 5.4.2 show the results from two flight lines with moderate ionospheric activity – T1002 and T1004 on April 19, respectively. The amount of improvement was quite small, and limited statistical testing showed that the differences between the carrier and position methods were not significant at a 95% confidence level. This was expected, given the conceptual similarity of the two methods of acceleration determination presented in Section 4. 5. However, the carrier method results from all the flight lines in the moderate and high ionospheric activity groups either matched the position method results or showed an improvement, albeit slight, at every filtering period. If the differences were due only to the noise level, one would expect the results to be worse as often as they were better.

Table 5.4.2 Errors (1 σ) of estimated δg_u with respect to the reference field (mGal) for T1004 flown on April 19, 2000: ionospheric variation = 0.06^2 m^2

Method	30s	60s	90s	120s
Carrier	21.59	3.10	1.23	0.98
Position	21.99	3.11	1.39	1.09

When the ionospheric variation was low, the carrier results were not consistently better over all filtering periods, as seen in the results from T1002 and T1001 on May 4 given in Tables 5.4.3 and 5.4.4, respectively.

Table 5.4.3 Errors (1 σ) of estimated δg_u with respect to the reference field (mGal) for T1002 flown on May 4, 2000: Ionospheric Variation = 0.03^2 m^2

Method	30s	60s	90s	120s
Carrier	8.32	1.66	1.24	1.16
Position	7.43	2.47	1.30	1.17

Table 5.4.4 Errors (1 σ) of estimated δg_u with respect to the reference field (mGal) for T1001 flown on May 4, 2000: Ionospheric Variation = 0.03^2 m^2

Method	30s	60s	90s	120s
Carrier	9.77	2.28	1.69	1.54
Position	9.99	2.27	1.51	1.46

It can be seen from Table 5.4.3 that the carrier method performed worse than the position method at the 30s filtering period, while Table 5.4.4 shows poorer carrier method performance over the longer filtering periods. Again, the difference in the performance of the carrier and position methods is small and arguably not significant. However, it is of note that carrier method results from periods of high ionospheric activity are always equal to or better than the position method. During periods of low ionospheric activity, the performance trend of the carrier method from the higher ionospheric conditions does not continue.

The T1001 of May 4 flight line had optimal conditions for GPS positioning. The ionospheric activity was extremely low. The PDOP was nearly constant at 1.06, with nine satellites available throughout the flight, with three satellites having elevations above 45˚. The appropriateness of the covariance model under these conditions was questioned. With such low ionospheric activity, the physical correlation between measurements may have been insignificant. However, the line was reprocessed without the covariance model, and results did not improve.

On the other hand, when conditions were less than optimal for GPS positioning, the carrier method provided better results than the position method. For example, during

T1002 of April 19, a maximum of six satellites was available throughout the flight line. Five satellites had elevations of less than 45˚. PDOP values ranged from 1.29 to 1.80. The greater percentage of low elevation satellites, combined with a higher level of ionospheric activity, created undesirable positioning conditions, which shows in the relatively poorer results of the position method. The relationship between the level of ionospheric activity and the performance of the carrier method is discussed further in Section 5.6.

5.5 Effect of Differentiator Bandwidth

To further examine the performance of the carrier method on T1001 of May 4, the differentiator bandwidths were investigated. In the carrier method, a fifth-order Taylor differentiator was used, which has a cut-off frequency of approximately 0.3 Hz. The differentiator in the position method had a cut-off frequency close to 0.1 Hz.

Initially, it was suspected that the differences between the two methods of acceleration determination were due mainly to the bandwidths of the differentiators. Since the flights from April 19 experienced moderate turbulence, it follows that a differentiator with a higher cut-off frequency could better capture higher frequency motion of the aircraft. Conversely, during the May 4 flights, which had minimal turbulence, the wider bandwidth would merely pass more noise, resulting in the carrier method's poorer performance.

To test this, the fifth-order Taylor differentiator was implemented in the position method. If the bandwidth argument was correct, the position method should then perform better during the turbulent flights, like T1002 of April 19, and worse during the smooth flights, as in T1001 of May 4. In fact, this was not the case. Tables 5.5.1 and 5.5.2 show the results from the carrier method and the position method using the fifth-order Taylor differentiator, along with the results from the position method using the standard differentiator, for comparison.

Table 5.5.1 Errors (1 σ) of estimated δg_u with respect to the reference field (mGal) for T1002 flown on April 19, 2000: the (*) on the first position method results indicates the use of the fifth-order Taylor differentiator

Method	30s	60s	90s	120s
Carrier	9.28	2.63	1.64	1.38
Position*	11.70	3.65	2.51	1.98
Position	11.26	2.73	1.88	1.53

Table 5.5.2 Errors (1 σ) of estimated δg_u with respect to the reference field (mGal) for T1001 flown on May 4, 2000: the (*) on the first position method results indicates the use of the fifth-order Taylor differentiator

Method	30s	60s	90s	120s
Carrier	9.77	2.28	1.69	1.54
Position*	9.99	2.26	1.53	1.47
Position	10.00	2.26	1.52	1.46

Increasing the differentiator bandwidth in the position method worsened the solution during the turbulent T1002 flight on April 19 and made very little difference to the results from the smooth T1001 flight of May 4. From these results, it can be concluded that the difference in performance between the carrier and position methods is not due to the bandwidth of the applied differentiators. This conclusion is valid when both applied differentiators are a good approximation of the ideal differentiator over the frequency range containing aircraft motion. A differentiator with a very narrow bandwidth would cause significant performance differences.

5.6 Discussion of Results

In the previous sections, it has been shown that:

- Low accuracy positions, up to 10 meters, can be used in the carrier method to produce the same results as when positions accurate to the decimeter level are used.

- A unique solution is not recommended for either method, because achievable accuracy is lower. In this situation, the carrier method can provide better accuracies than the position method, but it is very sensitive to errors in the carrier phase derivatives; therefore, the carrier method is not reliable when only four satellites are available.
- The carrier method can accommodate changes in geometry without adversely impacting the estimated accelerations.
- The carrier method performs better than the position method in less than optimal positioning conditions, in particular during increased ionospheric activity and with a majority of low elevation satellites.
- Differences in differentiator bandwidth do not explain the differences between the carrier and position methods of acceleration estimation.

The first two points will be briefly discussed first. The last three points are closely related and require further discussion to explain the observed performance of both methods under conditions of changing geometry and varying levels of ionospheric activity, along with differences in differentiator bandwidth.

To begin, it has been shown that poor quality positions yield acceleration results equivalent to higher quality positions. The testing verified the expected result, as the receiver and satellite positions are only used to compute the direction of the vector between them. This allows for simplified position processing, with required accuracies at the same level as for the normal gravity computation. This is only true if the low quality positions are due to the processing scheme, not the signal quality. Good signal quality is essential to both methods. Errors in the range accelerations, derived from the carrier phases, translate directly into the receiver acceleration estimates, but can be minimized in the least squares process.

When only four satellites are available, errors in the range accelerations from one satellite can cause very large errors in the acceleration estimates, as there is no opportunity for error minimization. Measurements to one additional satellite are sufficient to mitigate the

errors seen in the unique case. Therefore, the carrier method is considered reliable with five or more satellites only. Neglecting the "spiking" incidences, the carrier method performed better than the position method when the satellite set was restricted to four, inferring it is a better choice during low, but not minimal, availability.

The covariance model was shown to be critical to the carrier method's tolerance of changing satellite geometry. When satellite availability is low, introducing or losing a satellite causes large errors when the covariance model is not applied in the acceleration estimation. Conversely, when many satellites were used in the solution, the effect of visible constellation changes was more subtle. Even in this case, errors were reduced when the covariance model is used. These results can be explained from a least squares perspective. If measurements are equally weighted, each contributes very little when many are available. With few available measurements, the contribution of each is much larger, and not taking differences in quality into account in the weighting process will skew the estimated solution.

These observations based on the carrier method results imply that the difficulties in the position method due to geometry changes could also be overcome by applying a more appropriate covariance model. The jumps in the position solution when a satellite is gained or lost are very similar to the upsets in the carrier method acceleration solution when no covariance model is applied.

Recall the conceptual similarity between both methods presented in Section 4.5. The position method and the carrier method are essentially the same signal processing scheme, with the order of the filters switched. It has been shown in Section 5.5 that when applying the same differentiator in both the position method and carrier method, the results differ. Therefore, the differences must come from the least squares estimation processes. However, if both least squares estimation processes were equivalent, there should be no significant difference between the results of either method.

One difference between the position least squares estimation and the acceleration least squares estimation is the covariance model. In most commercial GPS processing packages, the position least squares estimation puts the emphasis on correcting errors, rather than modeling their variances. A troposphere model is applied and double differencing reduces remaining atmospheric errors. Unless an ionospheric free solution is utilized, the ionospheric errors remain unmodeled. The measurements are assumed to be independent, with only mathematical correlations taken into account. When the measurement conditions do not match the assumptions of the covariance model, the minimization of errors may not be done correctly. This would explain the jumps in the position trajectory when the satellite constellation changes, and the degraded position solutions after the inclusion of low elevation satellites.

The acceleration least squares estimation uses a satellite elevation angle based covariance model that incorporates physical correlations between measurements due to ionospheric and tropospheric variances. This covariance model appears to be more appropriate, as low elevation satellites can be included in the solution and poor geometry can be tolerated without negative effects. Differentiating the carrier phases removes constant and first order terms. Combined with double differencing, this process provides the justification for not applying corrections from a troposphere model. An ionospheric free solution, with L1 and L2, can only remove first order effects of the ionosphere, which differentiation already does, generating an effectively ionospheric free solution.

The covariance model influences how well the errors are minimized in the least squares estimation. When conditions match the assumptions made in the covariance model in the position estimation, the resulting solution has optimally minimized errors. If the conditions are less than ideal, the minimization of errors is not done correctly, producing a poorer quality position solution. The former situation occurs in the T1001 flight of May 4, which has low ionospheric activity, and the latter in the T1002 flight of April 19, which has high ionospheric activity. Also during the T1001 flight of May 4, which was very smooth, the application of a wider bandwidth differentiator did not significantly increase the error of the estimated gravity disturbance. In the turbulent T1002 flight of

April 19, the wider bandwidth differentiator significantly increased the errors. This implies that if the minimization of errors in the position solution is optimal, an increased differentiator bandwidth will not increase the noise level of the gravity disturbances.

The question remains as to why the carrier method, even with its more appropriate covariance model, performed worse than the position method on T1001 of May 4. Given the explanation above, the carrier method should have been able to at least match the performance of the position method. What was not mentioned before is that the position estimation is not purely a least squares estimation which uses measurements from the current epoch alone, like the acceleration least squares estimation is. The carrier phase ambiguities are estimated with a Kalman Filter, meaning all measurements since the initialization of the filter contribute to the estimate. The position vector is estimated using these ambiguity estimates, allowing each epoch's position solution to utilize more information than what is available at the current epoch. The acceleration estimation does not have the benefit of any information or measurement beyond the current epoch. For this reason, when the assumptions of its covariance model are correct and measurement conditions are ideal, the position method can perform better than the carrier method.

The common limiting factor in both the position and carrier method of acceleration estimation is the noise level of the GPS measurements. Double differencing is required in both methods. Schwarz and Wei (1994) identified carrier phase noise to be the dominant error in higher frequencies from 0.005 to 0.02 Hz, which corresponds to resolutions of 1.1 km to 4.5 km, with a 45 m/s flying speed. The carrier method, while offering operational advantages, does not offer the amount of accuracy improvement needed to meet the requirements of high-resolution geophysical applications. The same measurements are used in both the carrier and position methods, which are conceptually equivalent. The carrier method is hampered by the carrier phase noise in the same way that the position method is, preventing GPS derived accelerations from providing the desired accuracy at high frequencies.

In summary, the carrier method performs slightly better than the position method when measurement conditions are less than ideal. This improved performance is due to the carrier method's more appropriate covariance model. Theoretically, both the carrier method and the position method should yield equivalent results if the least squares estimation in both were equivalent. The carrier method requires good quality carrier phase measurements, but can tolerate position error of up to 10 meters. When only four satellites are available, the carrier method generally provides better acceleration estimates than the position method does, shown by the lower error level in estimated gravity disturbances. It is still not recommended in this case as the carrier method appears to be quite sensitive to a unique solution, when small errors in the carrier phase measurements occasionally cause large errors in the acceleration estimates. The carrier phase method is recommended if there is a minimum of five satellites available, which eliminates the incident of extreme outliers in the acceleration estimates. Ultimately, the carrier method is based upon the same GPS phase measurements, with the same noise level, as the position method. The position method and the carrier method will share the same upper bound in high frequency performance, because the noise level of the carrier phase measurements becomes the dominant error source in this part of the frequency spectrum.

5.7 Strengths and Limitations of the Modified Carrier Method

The results and discussion presented previously in this chapter have shown that using the modified carrier method has operational and algorithmic advantages over the position method. However, the amount of accuracy improvement is not enough to achieve the accuracies required for high-resolution geophysical applications. Therefore, the strength of the carrier method lies in its operational advantages. It offers the same quality of accelerations, or slightly better, with more straightforward processing, when five or more satellites are available.

Processing positions for use in the position method entails careful control of which satellites are used. This requires much input from the user, who must examine the status of each satellite, avoid constellation changes, and keep the elevation mask high enough to avoid inclusion of lower quality, low elevation satellites. Operationally, this is time

consuming, and also reduces the total number of usable satellites, which in some instances may lead to a unique solution, which is not desirable. Since the modified carrier method can accommodate constellation changes, and benefits from the inclusion of all available satellites, it can be implemented without such a high level of user input. Moreover, a differential code solution is all that is required for positions, meaning less sophisticated software can be utilized and ambiguity estimation is not required.

In the modified carrier method, the acceleration estimate comes directly from carrier phase derivatives. The effect of individual satellites on the acceleration solution can be easily identified. For example, during processing for T1004 of May 4, it was observed that the addition of PRN 3 worsened the solution. Upon investigation of the GPS satellite status advisories provided by the United States Coast Guard Navigation Center, it was discovered that PRN 3 had been unavailable for use, due to forecast maintenance, until just a few hours previous. Re-processing without PRN 3 improved the solution, inferring that this PRN may still have been experiencing effects from its "unusable" period. In the case of poor signal quality from a satellite, the modified carrier method allows for easy identification and removal of that satellite. Individual signal variances are propagated directly into the acceleration solution. With the position method, errors caused by one satellite's contribution are first mapped into the position domain and then differentiated into the acceleration domain, making the exact source of those errors less obvious in the acceleration estimate.

While the modified carrier method offers advantages in terms of simplified processing, and ease of variance propagation, it does have limitations. Firstly, cycle slips are a concern, just as in carrier phase positioning. The sharp discontinuity caused by a cycle slip causes edge effects in the carrier phase derivative. Cycle slips must be detected, and either fixed or the flight line must be broken into two segments at the cycle slip. (The edge effects will last the length of the differentiating filter, and then be further spread by the low pass filter applied to the gravity estimates.) Fixing cycle slips is not a trivial matter, and must be done correctly. An improper cycle slip fix will cause incorrect acceleration estimates, as shown in Section 3.4, again causing edge effects in the gravity

disturbance estimates. However, it should be kept in mind that the dynamics of airborne gravimetry flights are quite smooth and cycle slips are not common. Raw Doppler measurements could potentially be used to avoid the cycle slip problem. Since the accuracy of the relative velocity estimates is not crucial, the Doppler measurements from the receiver could be used as the first carrier phase derivative. The range accelerations would need to be derived from the raw Doppler measurements, with a low pass filtering scheme to meet the low error requirement on the range accelerations. This approach needs further investigation before it can be recommended.

Secondly, the modified carrier method requires either careful receiver selection or extra data processing due to receiver clock resets. As explained in Section 3.2, the problem with receiver clock offsets comes when differentiating the carrier phase measurements. An FIR differentiator requires uniformly spaced samples. When the receiver clock resets to GPS time, the sample spacing cannot be considered uniform if the reset is large. If the reset is large, the integration period over which the carrier phase measurement is formed is shorter or longer than the nominal output rate by the amount of the receiver clock offset. This results in the carrier phase measurement being either too large or too small by the amount of the receiver clock offset multiplied by the Doppler. This effect can be corrected in the same way as a cycle slip, with the time and magnitude of the receiver clock reset known.

The final limitation of the carrier phase method is its instability when using a unique solution. Although caution should also be exercised when using the position method with only four satellites, the effects are not as large in this case.

From the data processed herein, and the accompanying analysis, the carrier phase method is recommended:

- During conditions of low, but not minimal, satellite availability
- When the majority of available satellites are below 45 degrees elevation
- During periods of moderate to high ionospheric activity

- When satellites are introduced or lost during a flight period
- When the direct effect of individual satellite signals on acceleration have to be analyzed.

The position method, used with commercial GPS positioning packages and the current GPS constellation, is recommended:

- During ideal positioning conditions: low ionospheric activity, majority of available satellites having high elevation, and good satellite availability

Chapter 6

Summary, Conclusions and Recommendations

To investigate whether higher accuracy GPS accelerations can be achieved, an alternative method for deriving accelerations from GPS has been presented and evaluated. This method estimates accelerations directly from carrier phase derivatives, and is based on the method presented in Jekeli and Garcia (1997). The original carrier method was expanded upon to incorporate a least squares solution and a covariance model. Tropospheric and ionospheric variances are modeled, as well as physical correlations between measurements due to these errors. This modified carrier method is an improvement over the original (ibid), resulting in higher accuracy acceleration estimates.

The modified carrier method was evaluated with respect to the current standard method of acceleration determination from GPS, which is twice differentiated positions. To provide a benefit to airborne gravimetry systems, the modified carrier method must be shown to be superior to the current method, either in terms of accuracy or in terms of operational or algorithmic advantages.

For a fair comparison, the position method and the modified carrier method were tested under identical, operational conditions. Data from an airborne gravimetry campaign flown over the Alexandria, Canada area in the spring of 2000 was used. A reference gravity field for the area, computed from ground gravity measurements, was available. The GPS data was processed using both methods to provide two sets of aircraft accelerations which were used to compute two sets of gravity disturbances. The estimated gravity disturbances were then compared to the reference gravity field. The differences between the two sets were due to the acceleration estimation method used, as all other error sources are shared. Comparison to the reference gave an accuracy check to verify whether the differences were improvements.

Eight flight lines, totaling nearly 720 km, were processed with both acceleration determination methods. The same four flight lines were flown on two days. The first day had less than optimal conditions: moderate flight turbulence was encountered, there were periods of low satellite availability, and the ionospheric activity was significant. The second day of flying was close to ideal: nearly no flight turbulence was experienced, and ionospheric activity was extremely low. These two days allowed for an excellent comparison of how the position method and the modified carrier method performed under varying conditions.

Analysis of the results provided the following conclusions:

1) The modified carrier method is superior to the original carrier method, in terms of achievable accuracy and robustness. This is due to the use of all available satellites, rather than being restricted to four, and to the covariance model employed.

2) As part of the development of the modified carrier method, it has been shown that carrier phase variances can be propagated through the differentiation process. The variance propagation technique presented is applicable to any FIR filter.

3) The use of an elevation based covariance model that models physical correlations between measurements due to tropospheric and ionospheric errors has proven to be effective in allowing the use of low elevation satellites, poor satellite geometry, and the introduction or loss of a satellite without degrading the acceleration solution.

4) The modified carrier method performs best during conditions of:
    a. moderate ionospheric activity
    b. low, but not minimal, satellite availability
    c. poor geometry, or a large percentage of low elevation satellites
    d. rising or falling satellites (i.e. geometry changes)

5) The position method performs best during conditions of:
    a. low ionospheric activity
    b. constant satellite constellation (no losses or gains during a flight period)
    c. good geometry, with a large percentage of high elevation satellites

6) Overall the modified carrier method provides a slight improvement (~5%) in the accuracy of accelerations derived from GPS over all filtering periods, with the largest improvements (~15% at 30s and 60s filtering periods) during less than optimal conditions, as described in 4). These improvements in accuracy are quite small, and statistically speaking they are not significant, but they are consistent during less than optimal conditions. The carrier method results being consistently better, though only slightly, is of note, as differences due purely to the noise level would be expected to be negative as often as they are positive.

7) The modified carrier method provides operational and algorithmic advantages over the position method:
    a. Satellites can be gained or lost without any adverse effect on the estimated accelerations.
    b. Low elevation satellites can be included in the acceleration solution without degrading accuracy.
    c. Lower accuracy positions used in the modified carrier method produce the same quality of results as higher accuracy positions. This eliminates the need for ambiguity resolution, and the sophisticated processing it entails.
    d. The effect of one satellite's signal on the solution can be directly seen, allowing for easy elimination of satellites with low signal quality, for instance in the case of poor satellite health.

8) For the reasons given in 7), the modified carrier method is recommended for use in operational airborne gravimetry campaigns. It is at the very least equivalent to

the position method in terms of accuracy. Additionally, the modified carrier method allows for less intensive monitoring of the GPS data processing.

9) With the current GPS constellation and available signals, accelerations from GPS do not provide the accuracy required for very high-resolution gravity field estimation. Less than 1mGal at 1 km resolution has not been reliably achieved with either the modified position method or the carrier method.

6.1 Recommendations

The problem of higher accuracy motion compensation in airborne gravimetry is not yet solved. Future research must still be directed to this area in order to achieve the desired resolutions. It is recommended that the following areas be considered:

1) The completion and availability of the Galileo Global Navigation Satellite System (GNSS) may provide new levels of positioning accuracy, particularly since the combination of GPS and Galileo will increase the number of observations available. More observations should lead to better acceleration estimates with the carrier method. The planned modernization of GPS will impact its performance as well, partly because it will provide access to more signals for observation. These two developments could increase the accuracy of both GPS positions and accelerations. Their effect should be examined within the context of airborne gravimetry.

2) An investigation into the availability and feasibility of alternative height sensors with a lower noise level than GPS measurements should be done.

3) Refinement of the covariance model used in the modified carrier method should be considered. Ideally, C/No or Signal to Noise Ratio (SNR) measures from the receiver could be incorporated to give a time varying indication of signal quality.

4) The statistics from the least squares solution could be used for quality control in an operational flight. This would be a first step towards providing accuracy measures of the estimated gravity disturbances in operational campaigns when no reference is available. Currently these could be provided, but would only reflect the geometry of the solution, since the tropospheric and ionospheric zenith values are constant. If the recommendation in 4) is realized, warnings based on temporal disturbances in signal quality could also be provided.

References

Bell, R.E., V.A. Childers, R.A. Arko, D.D. Blankenship and J.M. Brozena (1999). *Airborne Gravity and Precise Positioning for Geological Applications*. Journal of Geophysical Research, Vol. 104, No. B8, pp. 15,281-15,292.

Beyer, W.H. (1980). Handbook of Mathematical Sciences, 5th Edition, CRC Press, Florida, USA.

Brozena, J.M., G.L. Mader, and M.F. Peters (1989). Interferometric *Global Positioning System: Three-Dimensional Positioning Source for Airborne Gravimetry*. Journal of Geophysical Research, Vol. 94, No. B9, pp.12,153-12,162.

Brozena, J.M., and V.A. Childers (2000). *The NRL Airborne Geophysics Program*. International Association of Geodesy Symposia, Vol. 121, Schwarz (ed.), Geodesy Beyond 2000 – The Challenges of the First Decade, pp.125-129, Springer-Verlag, Berlin.

Bruton, A.M. (2000). *Improving the Accuracy and Resolution of SINS/DGPS Airborne Gravimetry.* Ph.D. Thesis, Report No. 20145, Department of Geomatics Engineering, University of Calgary, Calgary, Alberta.

Bruton, A.M., C.L. Glennie, and K.P. Schwarz (1999). *Differentiation for High-Precision GPS Velocity and Acceleration Determination*. GPS Solutions, Vol.2, No. 4, pp. 4-21.

Bruton, A.M., Y. Hammada, S. Ferguson, K.P. Schwarz, M. Wei, J. Halpenny (2001a). *A Comparison of Inertial Platform, Damped 2-axis Platform and Strapdown Airborne Gravimetry*. In Proceedings of The International Symposium on Kinematic Systems in Geodesy, Geomatics, and Navigation (KIS 2001), June 5-8, Banff, Canada.

Bruton, A.M., M. Kern, K.P. Schwarz, S. Ferguson, A. Simsky, K. Tennant, M. Wei, J. Halpenny, R. Langley, T. Beran, K. Keller, P. Mrstik, K. Kusevic, R. Faulkener (2001b). *On the Accuracy of Kinematic Carrier Phase DGPS for Airborne Mapping*. Geomatica, Vol. 55, No. 4, pp. 491-507.

Cannon, M.E., G. Lachapelle, M.C. Szarmes, J.M. Hebert, J. Keith, and S. Jokerst (1997). *DGPS Kinematic Carrier Phase Signal Simulation Analysis for Precise Velocity and Position Determination*. Journal of the Institute of Navigation, Vol. 44, No.2.

Childers, V.A., and R.E. Bell, and J.M. Brozena (1999). *Airborne Gravimetry: An Investigation of Filtering*. Geophysics, Vol.64, No.1, pp.61-69.

Collins, J.P. (1999). *Assessment and Development of a Tropospheric Delay Model for Aircraft users of the Global Positioning System.* Technical Report No. 203. The University of New Brunswick.

Czompo, J. (1993). *GPS Accuracy Test for Airborne Gravimetry*. In Proceedings of ION GPS-93, The Institute of Navigation, pp. 805-810.

Czompo, J. and S. Ferguson (1995). *Design Considerations for a New Scalar Gravity Meter for Airborne Surveys*. In Proceedings IAG Symposium G4 Airborne Gravity Field Determination, XXI General Assembly of the IUGG, July 2-14, Boulder, Colorado pp.13-21.

Ferguson, S., and Y. Hammada (2000). *Experiences with AIRGrav: Results from a New Airborne Gravimeter*. In Proceedings of the IAG International Syposium in Geodesy, Geoid, and Geodynamics 2000, July 31-August 4, Banff Canada.

Forsberg, R., A. Oleson, L. Bastos, A. Gidskehaug, U. Meyer, and L. Timmen (2000). *Airborne Geoid Determination*. Earth Planets Space, 52, p.863-866.

Glennie, C. (1999). *An Analysis of Airborne Gravity by Strapdown INS/DGPS*. Ph.D. Thesis, UCGE Report Number 20125, Department of Geomatics Engineering, University of Calgary, Calgary, Alberta.

Glennie, C., K.P. Schwarz, A.M. Bruton, R. Forsberg, A.V. Oleson, and K. Keller (2000). *A Comparison of Stable Platform and Strapdown Airborne Gravity*. Journal of Geodesy, 74, 5, pp.383-389.

Hartinger, H. and F.K. Brunner (1999). *Variances of GPS Phase Observations: The Sigma-ε Model*. GPS Solutions, Vol.2, No.4, pp.35-43.

Hein, G.W. (1995). *Progress in Airborne Gravimetry Solved, Open, and Critical Problems*. In Proceedings IAG Symposium G4 Airborne Gravity Field Determination, XXI General Assembly of the IUGG, July 2-14, Boulder, Colorado, pp. 3-11.

Hoffmann-Wellenhof, B.H. Lichtenegger, and J.Collins (2001). *GPS Theory and Practice 5th Edition*. Springer-Verlag Wein, New York.

Jekeli, C. (1994). *On the Computation of Vehicle Accelerations Using GPS Phase Accelerations.* In Proceedings of the International Symposium on Kinematic Systems in Geodesy, Geomatics, and Navigation (KIS94), August 30-September 2, Banff, Canada, pp. 473-481.

Jekeli, C. and R. Garcia (1997). *GPS Phase Accelerations for Moving-base Vector Gravimetry*. Journal of Geodesy, 71, pp. 630-639.

Johnson, E.A.E. (1998). *Gravity and Magnetic Analyses Can Address Various Petroleum Issues*. The Leading Edge, January.

Kennedy, S.L., A.M. Bruton, and K.P. Schwarz (2001). *Improving DGPS Accelerations for Airborne Gravimetry: GPS Carrier Phase Accelerations Revisited*. In Proceedings of IAG 2001 Scientific Assembly, September 2-7, Budapest, Hungary.

Kleusberg, A., D. Peyton, and D. Wells (1990). *Airborne Gravimetry and the Global Positioning System*. In Proceedings of IEEE 1990, pp.273-278.

Mikhail, E.M. (1976). Observations and Least Squares. Dun-Donnelley Publisher, New York, USA.

NRC (National Research Council) (1995). *Airborne Geophysics and Precise Positioning: Scientific Issues and Future Direction*. In Proceedings of the Workshop on Airborne Geophysics, July 12-14, 1993, Washington, D.C., National Academy Press.

Peyton, D.R. (1990). *An Investigation into Acceleration Determination for Airborne Gravimetry Using the Global Positioning System*. M.Sc. Thesis, Report No.149, Department of Surveying Engineering, University of New Brunswick, Fredericton, N.B.

Olesen, A.V., R. Forsberg, and A. Gidskehaug (1997). *Airborne Gravimetry using the LaCoste and Romberg Gravimeter – An Error Analysis.* In Proceedings of the International Symposium on Kinematic Systems in Geodesy, Geomatics and Navigation (KIS97), Banff, Alberta, Canada, June 3 – 6, pp. 613-618.

Oppenheim, A.V. and R.W. Schafer (1999). Discrete-Time Signal Processing, 2nd Edition, Upper Saddle River, New Jersey, Prentice-Hall.

Parkinson, B.W. and J.J. Spilker (eds) (1996). *Global Positioning System: Theory and Applications*, American Institute of Aeronautics and Astronautics Inc., (2 volumes).

Racquet, J. (1998). *Development of a Method for Kinematic GPS Carrier-Phase Ambiguity Resolution Using Multiple Reference Receivers*. Ph.D. Thesis, UCGE Report No. 20116, Department of Geomatics Engineering, University of Calgary, Calgary, Alberta.

Radovanovic, R., N. El-Sheimy, and W.F. Teskey (2001). *Rigorous Network Adjustment of GPS Carrier Phases for Airborne Positioning via Tropospheric Error Variance-Covariance.* In Proceedings of the 3rd International Mobile Mapping Conference, January 3-10, Cairo, Egypt.

Ryan, R., G. Lachapelle, and M.E. Cannon (1997). *DGPS Kinematic Carrier Phase Signal Simulation Analysis in the Velocity Domain*. In Proceedings of ION GPS 97, September 16-19, Kansas City, Missouri.

Salychev, O.S. and K.P. Schwarz (1995). *Airborne Gravimetric Results Obtained with the ITC-2 Inertial Platform System.* In Proceedings IAG Symposium G4 Airborne

Gravity Field Determination, XXI General Assembly of the IUGG, July 2-14, Boulder, Colorado, pp.125-141.

Shaw, M., K. Sandhoo, and D. Turner (2000). *Modernization of the Global Positioning System*. GPS World, Vol.11, No. 9, pp. 36-44.

Schwarz, K.P. O. Colombo, G. Hein, and E.T. Knickmeyer (1991). *Requirements for Airborne Vector Gravimetry*. In Proceedings of the IAG Symposium No. 110, From Mars to Greenland: Charting with Space and Airborne Instruments, Springer Verlag. New York, pp. 273-283.

Schwarz, K.P. and M.Wei (1994). *Some Unsolved Problems in Airborne Gravimetry.* IAG Symposium 'Gravity and Geoid', September 11-17, Graz, Austria, pp.131-150.

Schwarz, K.P. and Y.C. Li (1996a). *What Can Airborne Gravimetry Contribute to Geoid Determination?* Journal of Geophysical Research, Vol.101, No. B8, pp.17,873 -17, 881.

Schwarz, K.P. and Z. Li (1996b). *An Introduction to Airborne Gravimetry and its Boundary Value Problems*. Lecture Notes IAG Summer School, May 26 – June 7, Como, Italy.

Skone, S. (1998). *An Adaptive WADGPS Ionospheric Gird Model for the Auroral Region*. In Proceedings of the ION-98, the 11th International Technical Meeting of the Satellite Division of the Institute of Navigation, Septemeber 15-19, Nashville, Tennessee, pp. 185-194.

Szarmes, M., S. Ryan, G. Lachapelle and P. Fenton (1997). *DGPS High Accuracy Aircraft Velocity Determination Using Doppler Measurements*. In Proceedings of the International Symposium on Kinematic Systems (KIS97), June 3-6, Banff, Alberta, Canada.

Van Dierendonck, K.J., M.E. Cannon, M. Wei, and K.P. Schwarz (1994). *Error Sources in GPS-Determined Acceleration for Airborne Gravimetry*. In Proceedings of ION Technical Meeting, January 24-26, San Diego, CA, pp.811-820.

Wei, M., S. Ferguson, and K.P. Schwarz (1991). *Accuracy of GPS-Derived Acceleration From Moving Platform Tests*. In Proceedings of IAG Symposium No.110, From Mars to Greenland: Charting with Space and Airborne Instruments, Springer Verlag, New York, pp. 235-249.

William, S. and J.D. MacQueen (2001). *Development of a Versatile, Commercially Proven and Cost-Effective Airborne Gravity System*. The Leading Edge, June 2001.

Appendix A

Results with the Modified Carrier Method and Flight Line Data

The following tables contain the error of the estimated gravity disturbances, using the modified carrier method, with respect to the reference field, low pass filtered with cut-off frequencies corresponding to the time periods given. These results are the best attained, using high quality positions, all available satellites and the covariance model developed. Information about each flight line is also provided. The mean ionospheric variance is calculated as described in section 5.4. The turbulence measures were taken from the pilot's notes.

Flight Line:	**T1001 April 19, 2000**
Flight Time:	317674 – 319750 (GPS seconds of week)
	11:14 – 11:49 (Local time)
Mean Ionospheric Variance:	0.13^2 m^2
Turbulence:	Moderate
Total Number of Available PRNs:	7
Gains:	0
Losses:	PRN 8 at 318421
Average PDOP:	1.18
Average VDOP:	0.67

Table A.1 Available PRNs and average elevation angles for T1001 of April 19, 2000

PRN	*Average Elevation (^{o})*
2	75
4	25
7	65
8	12
9	16
11	28
16	20

Table A.2 Errors (1 σ) of estimated δg_u with respect to reference (mGal), calculated with accelerations from the modified carrier method, for T1001 of April 19, 2000

Method	**30s**	**60s**	**90s**	**120s**
Modified Carrier, all available satellites	10.58	3.95	3.30	3.06

Flight Line:	**T1002 April 19, 2000**
Flight Time:	320414 – 322094 (GPS seconds of week)
	12:00 – 12:39(Local time)
Mean Ionospheric Variance:	0.06^2 m^2
Turbulence:	Moderate
Total Number of Available PRNs:	7
Gains:	PRN 24 at 321853
Losses:	PRN 11 at 321834
Average PDOP:	1.55
Average VDOP:	0.77

Table A.3 Available PRNs and average elevation angles for T1002 of April 19, 2000

PRN	*Average Elevation (^{o})*
2	55
4	45
7	77
9	20
11	12
16	37
24	10

Table A.4 Errors (1 σ) of estimated δg_u with respect to reference (mGal), calculated with accelerations from the modified carrier method, for T1002 of April 19, 2000

Method	**30s**	**60s**	**90s**	**120s**
Modified Carrier, all available satellites	9.28	2.63	1.64	1.38

Flight Line:	**T1003 April 19, 2000**
Flight Time:	332174 – 334472 (GPS seconds of week)
	15:16 – 15:54 (Local time)
Mean Ionospheric Variance:	0.06^2 m^2
Turbulence:	Moderate
Total Number of Available PRNs:	11
Gains:	PRN 6 at 332748
Losses:	PRN 1 at 333353
	PRN 7 at 333473
	PRN 16 at 332995
Average PDOP:	1.08
Average VDOP:	0.56

Table A.5 Available PRNs and average elevation angles for T1003 of April 19, 2000

PRN	*Average Elevation (^{o})*
1	10
4	45
5	30
6	15
7	15
10	53
13	29
16	12
18	30
24	75
30	30

Table A.6 Errors (1 σ) of estimated δg_u with respect to reference (mGal), calculated with accelerations from the modified carrier method, for T1003 of April 19, 2000

Method	**30s**	**60s**	**90s**	**120s**
Modified Carrier, all available satellites	27.74	4.84	1.97	1.52

Flight Line:	**T1004 April 19, 2000**
Flight Time:	329367 – 331641 (GPS seconds of week)
	14:29 – 15:07 (Local time)
Mean Ionospheric Variance:	0.06^2 m^2
Turbulence:	Moderate
Total Number of Available PRNs:	9
Gains:	PRN 13 at 330197
Losses:	0
Average PDOP:	1.09
Average VDOP:	0.59

Table A.7 Available PRNs and average elevation angles for T1004 of April 19, 2000

PRN	*Average Elevation (^{o})*
1	16
4	60
5	38
7	30
10	30
13	12
16	25
24	65
30	21

Table A.8 Errors (1 σ) of estimated δg_u with respect to reference (mGal), calculated with accelerations from the modified carrier method, for T1004 of April 19, 2000

Method	**30s**	**60s**	**90s**	**120s**
Modified Carrier, all available satellites	21.59	3.10	1.23	0.98

Flight Line:	**T1001 May 4, 2000**
Flight Time:	388329 – 390337 (GPS seconds of week)
	06:52 – 07:25 (Local time)
Mean Ionospheric Variance:	0.03^2 m^2
Turbulence:	Low
Total Number of Available PRNs:	9
Gains:	0
Losses:	PRN 18 at 389747
Average PDOP:	1.06
Average VDOP:	0.57

Table A.9 Available PRNs and average elevation angles for T1001 of May 4, 2000

PRN	*Average Elevation (^{o})*
2	15
3	28
8	55
11	30
13	27
15	37
18	15
19	55
27	65

Table A.10 Errors (1 σ) of estimated δg_u with respect to reference (mGal), calculated with accelerations from the modified carrier method, for T1001 of May 4, 2000

Method	**30s**	**60s**	**90s**	**120s**
Modified Carrier, all available satellites	9.77	2.28	1.69	1.54

Flight Line:	**T1002 May 4, 2000**
Flight Time:	385721 – 387602 (GPS seconds of week)
	06:08 – 06:40 (Local time)
Mean Ionospheric Variance:	0.03^2 m^2
Turbulence:	Low
Total Number of Available PRNs:	9
Gains:	PRN 11 at 386359
Losses:	0
Average PDOP:	1.27
Average VDOP:	0.59

Table A.11 Available PRNs and average elevation angles for T1002 of May 4

PRN	*Average Elevation (^{o})*
3	46
8	35
11	14
13	30
15	28
18	29
19	75
22	16
27	49

Table A.12 Errors (1 σ) of estimated δg_u with respect to reference (mGal), calculated with accelerations from the modified carrier method, for T1002 of May 4, 2000

Method	**30s**	**60s**	**90s**	**120s**
Modified Carrier, all available satellites	8.32	1.66	1.24	1.16

Flight Line:	**T1003 May 4, 2000**
Flight Time:	382924 – 385046 (GPS seconds of week)
	05:21 – 05:57 (Local time)
Mean Ionospheric Variance:	0.05^2 m^2
Turbulence:	Low
Total Number of Available PRNs:	9
Gains:	PRN 15 at 383682
Losses:	0
Average PDOP:	1.14
Average VDOP:	0.57

Table A.13 Available PRNs and average elevation angles for T1003 of May 4, 2000

PRN	*Average Elevation (^{o})*
1	35
3	60
8	16
13	23
15	15
18	40
19	75
22	32
27	30

Table A.14 Errors (1 σ) of estimated δg_u with respect to reference (mGal), calculated with accelerations from the modified carrier method, for T1003 of May 4, 2000

Method	**30s**	**60s**	**90s**	**120s**
Modified Carrier, all available satellites	6.28	2.38	2.02	1.89

Flight Line:	**T1004 May 4, 2000**
Flight Time:	381270 – 382251 (GPS seconds of week)
	04:55 – 05:11 (Local time)
Mean Ionospheric Variance:	0.03^2 m^2
Turbulence:	Low
Total Number of Available PRNs:	7
Gains:	PRN 13 at 380316
Losses:	0
Average PDOP:	1.79
Average VDOP:	0.58

Table A.15 Available PRNs and average elevation angles for T1004 of May 4, 2000

PRN	*Average Elevation (^{o})*
1	50
3	62
13	11
18	47
19	55
22	47
27	15

Table A.16 Errors (1 σ) of estimated δg_u with respect to reference (mGal), calculated with accelerations from the modified carrier method, for T1004 of May 4, 2000

Method	**30s**	**60s**	**90s**	**120s**
Modified Carrier, all available satellites	8.05	2.59	1.49	0.84

Appendix B

Results with the Unique Carrier Phase Method

The following tables contain the error of the estimated gravity disturbances, using the unique carrier phase method, with respect to the reference field, low pass filtered with cut-off frequencies corresponding to the time periods given. These results were obtained with the set of four satellites indicated under each Table, along with the PDOP and VDOP values.

Flight Line: **T1001 April 19, 2000**

Table B.1 Errors (1 σ) of estimated δg_u with respect to reference (mGal), calculated with accelerations from the unique carrier method, for T1001 of April 19, 2000

Method	30s	60s	90s	120s
Carrier, 4 satellites	33.40	9.89	5.48	4.11

PRNs used: 4, 9, 11, 16

Average PDOP: 1.72

Average VDOP: 1.30

Flight Line: **T1002 April 19, 2000**

Table B.2 Errors (1 σ) of estimated δg_u with respect to reference (mGal), calculated with accelerations from the unique carrier method, for T1002 of April 19, 2000

Method	30s	60s	90s	120s
Carrier, 4 satellites	13.09	3.37	1.92	1.63

PRNs used: 2, 4, 7, 16

Average PDOP: 2.03

Average VDOP: 0.82

Flight Line: **T1003 April 19, 2000**

Table B.3 Errors (1 σ) of estimated δg_u with respect to reference (mGal), calculated with accelerations from the unique carrier method, for T1003 of April 19, 2000

Method	30s	60s	90s	120s
Carrier, 4 satellites	35.97	6.17	2.32	1.50

PRNs used: 4, 10, 18, 24

Average PDOP: 2.62

Average VDOP: 0.71

Flight Line: **T1004 April 19, 2000**

Table B.4 Errors (1 σ) of estimated δg_u with respect to reference (mGal), calculated with accelerations from the unique carrier method, for T1004 of April 19, 2000

Method	30s	60s	90s	120s
Carrier, 4 satellites	35.87	9.69	4.07	2.66

PRNs used: 1, 4, 16, 24

Average PDOP: 5.63

Average VDOP: 1.55

Flight Line: **T1001 May 4, 2000**

Table B.5 Errors (1 σ) of estimated δg_u with respect to reference (mGal), calculated with accelerations from the unique carrier method, for T1001 of May 4, 2000

Method	30s	60s	90s	120s
Carrier, 4 satellites	27.91	9.00	4.09	2.65

PRNs used: 2, 8, 13, 27

Average PDOP: 4.80

Average VDOP: 1.49

Flight Line: **T1002 May 4, 2000**

Table B.6 Errors (1 σ) of estimated δg_u with respect to reference (mGal), calculated with accelerations from the unique carrier method, for T1002 of May 4, 2000

Method	30s	60s	90s	120s
Carrier, 4 satellites	36.39	6.58	2.49	1.73

PRNs used: 8, 13, 19, 27

Average PDOP: 8.33

Average VDOP: 1.67

Flight Line: **T1003 May 4, 2000**

Table B.7 Errors (1 σ) of estimated δg_u with respect to reference (mGal), calculated with accelerations from the unique carrier method, for T1003 of May 4, 2000

Method	30s	60s	90s	120s
Carrier, 4 satellites	7.44	2.88	2.04	1.88

PRNs used: 3, 18, 19, 27

Average PDOP: 2.25

Average VDOP: 0.71

Flight Line: **T1004 May 4, 2000**

Table B.8 Errors (1 σ) of estimated δg_u with respect to reference (mGal), calculated with accelerations from the unique carrier method, for T1004 of May 4, 2000

Method	30s	60s	90s	120s
Carrier, 4 satellites	13.01	5.07	3.12	2.17

PRNs used: 1, 18, 19, 27

Average PDOP: 3.59

Average VDOP: 0.65

Appendix C

Results with the Position Method

The following tables contain the error of the estimated gravity disturbances, using the position method, with respect to the reference field, low pass filtered with cut-off frequencies corresponding to the time periods given. The position solution was obtained in widelane fixed mode, using GrafNav™. The positions were carefully processed to avoid visible constellation changes during the flight lines.

Flight Line: **T1001 April 19, 2000**

Table C.1 Errors (1 σ) of estimated δg_u with respect to reference (mGal), calculated from an acceleration solution derived from positions, for T1001 of April 19, 2000

Method	30s	60s	90s	120s
Position	10.49	4.06	3.37	3.13

Flight Line: **T1002 April 19, 2000**

Table C.2 Errors (1 σ) of estimated δg_u with respect to reference (mGal), calculated from an acceleration solution derived from positions, for T1002 of April 19, 2000

Method	30s	60s	90s	120s
Position	11.26	2.73	1.88	1.53

Flight Line: **T1003 April 19, 2000**

Table C.3 Errors (1 σ) of estimated δg_u with respect to reference (mGal), calculated from an acceleration solution derived from positions, for T1003 of April 19, 2000

Method	30s	60s	90s	120s
Position	27.76	4.81	2.00	1.52

Flight Line: **T1004 April 19, 2000**

Table C.4 Errors (1 σ) of estimated δg_u with respect to reference (mGal), calculated from an acceleration solution derived from positions, for T1004 of April 19, 2000

Method	30s	60s	90s	120s
Position	21.99	3.11	1.39	1.09

Flight Line: **T1001 May 4, 2000**

Table C.5 Errors (1 σ) of estimated δg_u with respect to reference (mGal), calculated from an acceleration solution derived from positions, for T1001 of May 4, 2000

Method	30s	60s	90s	120s
Position	9.99	2.27	1.51	1.46

Flight Line: **T1002 May 4, 2000**

Table C.6 Errors (1 σ) of estimated δg_u with respect to reference (mGal), calculated from an acceleration solution derived from positions, for T1002 of May 4, 2000

Method	30s	60s	90s	120s
Position	7.43	2.47	1.30	1.17

Flight Line: **T1003 May 4, 2000**

Table C.7 Errors (1 σ) of estimated δg_u with respect to reference (mGal), calculated from an acceleration solution derived from positions, for T1003 of May 4, 2000

Method	30s	60s	90s	120s
Position	8.85	3.07	2.23	1.95

Flight Line: **T1004 May 4, 2000**

Table C.8 Errors (1 σ) of estimated δg_u with respect to reference (mGal), calculated from an acceleration solution derived from positions, for T1004 of May 4, 2000

Method	30s	60s	90s	120s
Position	9.19	2.52	1.49	1.07

Appendix D

Results with the Unique Position Method

The following tables contain the error of the estimated gravity disturbances, using the unique position method, with respect to the reference field, low pass filtered with cut-off frequencies corresponding to the time periods given. The position solution was obtained in L1 float mode, using GrafNav™. The processing was restricted to the same set of four satellites used in the unique carrier method of acceleration determination.

Flight Line: **T1002 April 19, 2000**

Table D.1 Errors (1 σ) of estimated δg_u with respect to reference (mGal), calculated with unique position method accelerations, for T1002 of April 19, 2000

Method	30s	60s	90s	120s
Position, 4 satellites	16.86	6.59	5.09	4.11

PRNs used: 2, 4, 7, 16

Average PDOP: 2.03

Average VDOP: 0.82

Flight Line: **T1003 April 19, 2000**

Table D.2 Errors (1 σ) of estimated δg_u with respect to reference (mGal), calculated with unique position method accelerations, for T1003 of April 19, 2000

Method	30s	60s	90s	120s
Position, 4 satellites	35.66	6.21	2.24	1.61

PRNs used: 4, 10, 18, 24

Average PDOP: 2.62

Average VDOP: 0.71

Flight Line: **T1004 April 19, 2000**

Table D.3 Errors (1 σ) of estimated δg_u with respect to reference (mGal), calculated with unique position method accelerations, for T1004 of April 19, 2000

Method	30s	60s	90s	120s
Position, 4 satellites	23.29	4.34	2.28	1.77

PRNs used: 1, 4, 16, 24

Average PDOP: 5.63

Average VDOP: 1.55

Flight Line: **T1001 May 4, 2000**

Table D.4 Errors (1 σ) of estimated δg_u with respect to reference (mGal), calculated with unique position method accelerations, for T1001 of May 4, 2000

Method	30s	60s	90s	120s
Position, 4 satellites	51.35	16.12	6.54	4.29

PRNs used: 2, 8, 13, 27

Average PDOP: 4.80

Average VDOP: 1.49

Flight Line: **T1002 May 4, 2000**

Table D.5 Errors (1 σ) of estimated δg_u with respect to reference (mGal), calculated with unique position method accelerations, for T1002 of May 4, 2000

Method	30s	60s	90s	120s
Position, 4 satellites	28.22	8.23	5.66	5.26

PRNs used: 8, 13, 19, 27

Average PDOP: 8.33

Average VDOP: 1.67

Flight Line: **1003 May 4, 2000**

Table D.6 Errors (1 σ) of estimated δg_u with respect to reference (mGal), calculated with unique position method accelerations, for T1003 of May 4, 2000

Method	30s	60s	90s	120s
Position, 4 satellites	11.02	4.52	2.93	2.21

PRNs used: 3, 18, 19, 27

Average PDOP: 2.25

Average VDOP: 0.71

Flight Line: **T1004 May 4, 2000**

Table D.7 Errors (1 σ) of estimated δg_u with respect to reference (mGal), calculated with unique position method accelerations, for T1004 of May 4, 2000

Method	30s	60s	90s	120s
Position, 4 satellites	9.95	5.41	306	2.31

PRNs used: 1, 18, 19, 27

Average PDOP: 3.59

Average VDOP: 0.65

Appendix E

Results with the Modified Carrier Method Using Low Quality Positions

The following tables contain the error of the estimated gravity disturbances, using the modified carrier method with code positions, with respect to the reference field, low pass filtered with cut-off frequencies corresponding to the time periods given. GrafNav™ was used to compute a differential code solution for the positions. The estimated accuracy of the positions, as reported by GrafNav™, is approximately 3 – 5 meters.

Flight Line: **T1001 April 19, 2000**

Table E.1 Errors (1 σ) of estimated δg_u with respect to reference (mGal), calculated with carrier method aircraft accelerations using poor quality positions, for T1001 of April 19, 2000

Method	30s	60s	90s	120s
Modified Carrier, all available satellites	10.55	3.95	3.31	3.06

Flight Line: **T1002 April 19, 2000**

Table E.2 Errors (1 σ) of estimated δg_u with respect to reference (mGal), calculated with carrier method aircraft accelerations using poor quality positions, for T1002 of April 19, 2000

Method	30s	60s	90s	120s
Modified Carrier, all available satellites	9.27	2.62	1.64	1.38

Flight Line: **T1003 April 19, 2000**

Table E.3 Errors (1 σ) of estimated δg_u with respect to reference (mGal), calculated with carrier method aircraft accelerations using poor quality positions, for T1003 of April 19, 2000

Method	30s	60s	90s	120s
Modified Carrier, all available satellites	27.74	4.84	1.97	1.52

Flight Line: **T1004 April 19, 2000**

Table E.4 Errors (1 σ) of estimated δg_u with respect to reference (mGal), calculated with carrier method aircraft accelerations using poor quality positions, for T1004 of April 19, 2000

Method	30s	60s	90s	120s
Modified Carrier, all available satellites	21.57	3.10	1.23	0.98

Flight Line: **T1001 May 4, 2000**

Table E.5 Errors (1 σ) of estimated δg_u with respect to reference (mGal), calculated with carrier method aircraft accelerations using poor quality positions, for T1001 of May 4, 2000

Method	30s	60s	90s	120s
Modified Carrier, all available satellites	9.87	2.28	1.72	1.56

Flight Line: **T1002 May 4, 2000**

Table E.6 Errors (1 σ) of estimated δg_u with respect to reference (mGal), calculated with carrier method aircraft accelerations using poor quality positions, for T1002 of May 4, 2000

Method	30s	60s	90s	120s
Modified Carrier, all available satellites	8.34	1.69	1.24	1.16

Flight Line: **T1003 May 4, 2000**

Table E.7 Errors (1 σ) of estimated δg_u with respect to reference (mGal), calculated with carrier method aircraft accelerations using poor quality positions, for T1003 of May 4, 2000

Method	30s	60s	90s	120s
Modified Carrier, all available satellites	6.21	2.36	2.01	1.88

Flight Line: **T1004 May 4, 2000**

Table E.8 Errors (1 σ) of estimated δg_u with respect to reference (mGal), calculated with carrier method aircraft accelerations using poor quality positions, for T1004 of May 4, 2000

Method	30s	60s	90s	120s
Modified Carrier, all available satellites	8.09	2.46	1.45	0.87